Please cite as: Francioni, Mirko, Stead, Doug, Sciarra, Nicola, Calamita, Fernando (2018). A new approach for defining Slope Mass Rating in heterogeneous sedimentary rocks using a combined remote sensing GIS approach. BULLETIN OF ENGINEERING GEOLOGY AND THE ENVIRONMENT, ISSN: 1435-9529, doi: 10.1007/s10064-018-1396-1

A new approach for defining Slope Mass Rating in heterogeneous sedimentary rocks using a combined remote sensing GIS approach.

Mirko Francioni (a), Doug Stead (b), Nicola Sciarra (a), Fernando Calamita (a)

a) Department of Engineering and Geology, University "G. d'Annunzio" of Chieti-Pescara, Chieti, Italy

b) Department of Earth Sciences, Simon Fraser University, Burnaby, BC, Canada

Corresponding author: Mirko Francioni (mirko.francioni@unich.it). Via dei Vestini, 31, 66100 Chieti (CH). Italy.

Abstract

Engineering rock mass classification is usually the first stage in the analysis and characterization of rock slopes. However, when dealing with sedimentary/heterogeneous rock masses, the use of the existing classification methods can be difficult and often misleading, especially when used to define rockfall risk areas and appropriate slope mitigation works.

In this research, we describe a novel approach for geomechanical rock slope analysis based on the combined use of remote sensing, Geographical Information System (GIS) and the Slope Mass Rating (SMR) classification system. The Montagna dei Fiori area (Italian Central Apennines), which is characterized by the sedimentary rocks of the Umbria Marche heterogeneous succession, is used as a case study to demonstrate the application of the proposed approach.

Conventional geomechanical scanlines are integrated with photogrammetric techniques to increase the amount of data collected, especially in inaccessible areas. In particular, a new fast and low-cost method of geo-referencing 3D photogrammetric models is presented.

Geographic Information Systems are used to manage all the data acquired using remote sensing techniques and geomechanical analyses and a semi-automatic tool developed to allow calculation of the Slope Mass Rating along a major highway, the SP52, which crosses the study area.

Finally, a modification of the Slope Mass Rating procedure is proposed to enable definition of the most appropriate mitigation works in folded heterogeneous sedimentary rock masses comprising alternating marls and limestones.

Keywords: Geomechanical analysis, Photogrammetry, GIS, Rock mass classification, Slope Mass Rating, Rockfall hazard

1. Introduction

Rockfalls are a major hazard for human activities, especially in proximity of infrastructure such as roads, railways and housing. The study of rockfall events is complex and has been related to several factors including the geology and structural setting of the area, rainfall, earthquakes, vegetation etc. During investigations of rock slopes, engineering rock mass classification is commonly a part of the first stage in the engineering geological analyses undertaken. The use of engineering rock mass classifications can be important in varied situations, such as feasibility study for roads and/or tunnels and for understanding the rock mass quality of natural and engineered rock slopes. The most commonly used rock mass classification systems are the Rock

Mass Rating, RMR (Bieniawski, 1973, 1989), the NGI Q-system (Barton et al., 1974; Barton and Grimstad, 2014; NGI, 2015) and the Geological Strength Index, GSI (Hoek, 1994; Hoek et al., 1995: Hoek and Brown, 1997). Initially, both the RMR and the Q systems were developed for tunnel engineering and only subsequently, was the RMR adapted for slopes and foundations (Bieniawski, 1989). The use of RMR for slope analysis has continued to remain challenging and, in some cases even misleading; for this reason, Romana (1993), Romana et al. (2003), Romana et al. (2015) proposed a modification to the RMR system specifically suited to rock lopes. This method, endorsed by Bieniawski (1989, 1993) and named the Slope Mass Rating, SMR, is obtained from RMR by adding an adjustment factor related to the relative orientation of the joints and the slope. Using the SMR classification value and the joint volumetric count (Jv), Romana (1993) proposed engineering solutions for mitigating rockfall risk. Modifications of the SMR methods have been subsequently proposed by Chen (1995), Tomás et al. (2007), Tomás et al. (2012) and Pantelidis (2010). A review of such modified approaches is presented by Basahel and Mitri (2017) in the analyses of several rock slopes in a region of Saudi Arabia. Romana et al. (2013) published a thirty years review of the SMR system highlighting the advantages and the improvements introduced by this system.

The GSI method is inherently different from the above-mentioned rock mass classification systems and has been specifically developed to meet the requirements for reliable input data in the numerical analysis of rock slopes, underground excavations and foundations in rock (Hoek et al., 1995). GSI is based on the geological description of homogeneous and heterogeneous rock masses (Hoek and Brown, 1997; Hoek and Marinos, 2000; Marinos and Hoek, 2000; Marinos and Hoek, 2001) and can be subjective requiring considerable experience (Cai et al. 2004). To overcome this problem, Cai et al. (2004) and Hoek et al. (2013) proposed quantitative approaches based on the calculation of geomechanical indices to assist in the use of the GSI system. Recently, Day et al. (2014) and Day et al. (2016) proposed a modification to the Geological Strength Index (GSI), the Composite GSI (CGSI) approach, suitable for a more realistic estimation of strength in complex rock masses. Although the GSI is very simple and useful when slope numerical simulations are needed, it was not developed to provide preliminary information on possible slope mitigation works.

Bar and Barton (2017) recently developed the Q-Slope method for rock slope engineering. This classification is intended for reinforcement-free road or railway cuttings or open pit mines. The Q-slope method allows the engineer to make potential adjustments to slope angles in relation to the rock mass conditions. It represents a very powerful tool for geotechnical engineering during road cut and/or pit excavation but does not provide information on possible mitigation works to be used for unstable natural slopes or road cuts.

Many authors over recent decades have discussed the use of rock mass classifications (Hamidi et al., 2010; Yilmaz et al. 2012; Salvini et al., 2011, 2013, Jaques et al., 2015; Sciarra et al. 2015). Some examples in mining engineering have been documented by Jaques et al. (2015) showing the use of different classification systems in the Volta Grande underground mine (Brazil) and by Hamidi et al. (2010) who applied the RMR to predict the performance of TBM's. Salvini et al. (2011 and 2013) described the use of RMR and SMR in two natural slopes in Italy while Budetta et al. (2011) illustrated the application of the GSI to heterogeneous rock masses in Italy, characterized by sandstones alternating with argillaceous marls. Riquelme et al. (2016) documented the advantages of using remote sensing data in engineering rock mass characterization.

This paper presents a new approach for defining areas of rockfall risk and proposing suitable mitigation works in potentially unstable natural slopes and road cuts. The Montagna dei Fiori anticline, located in the Italian Central Apennines (Figure 1) and characterized by the sedimentary rocks of the Umbria Marche succession, is used as a case example. The proposed approach is based on a combination of remote sensing, GIS and the SMR. Remote sensing and GIS techniques are used to improve our understanding of the rock mass

characteristics. We outline a fast and low-cost photogrammetric methodology using a simple hand-held camera. This approach has been initially developed for the study of low-to-medium elevation slopes and is based on a simple procedure using a triangle of known geometry and a geological compass. Structure from Motion (SfM) techniques (Westoby et al. 2012) are utilized to create the 3D model of the slopes under study and a freeware software (GPL software, 2018) to identify and measure geological features. Remote sensing and geomechanical data are then integrated and analyzed using GIS techniques to define rockfall risk areas.

Finally, the importance of understanding the geological and structural evolution of the area will be discussed with a particular focus on the importance of considering the geological and structural model in the definition of possible failure mechanisms (Badger, 2002; Stead and Wolter, 2015) and the most appropriate mitigation works.

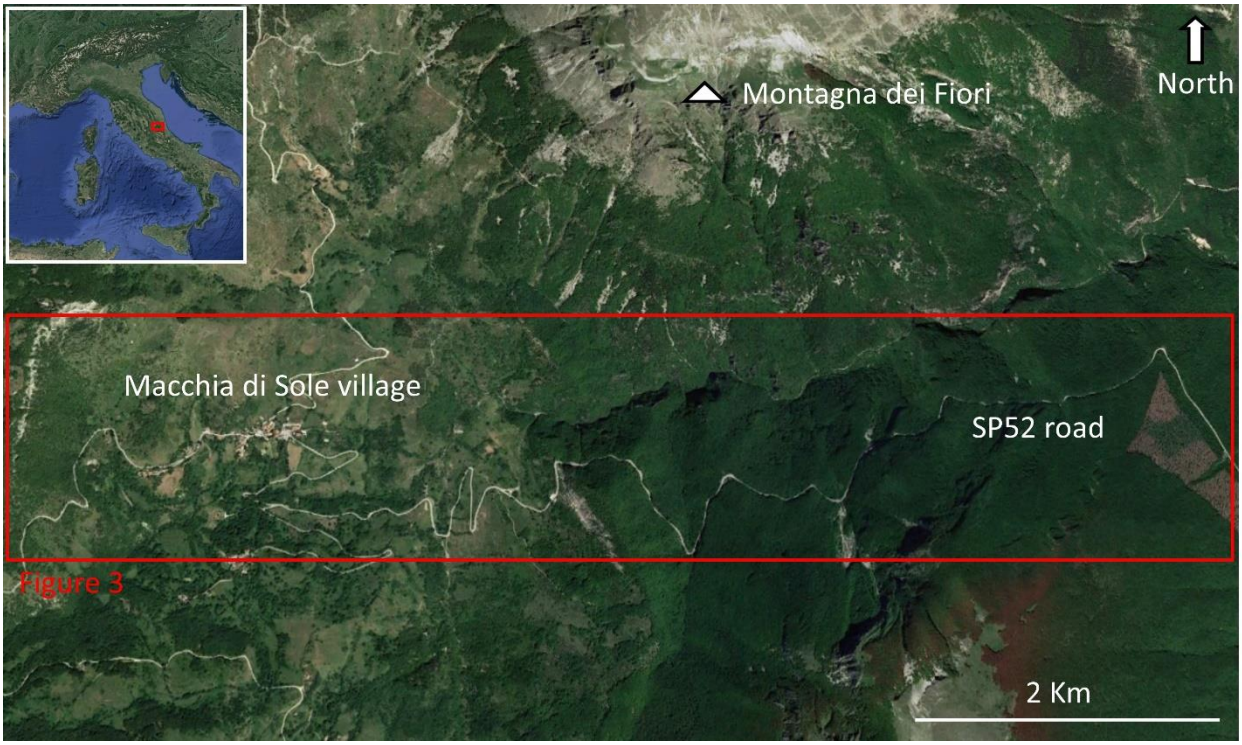

Figure 1. Location of the study area Montagna dei Fiori, Central Italy.

2. Study area

To illustrate the proposed approach, we use rock outcrops in the Montagna dei Fiori area in the Italian Central Apennines as case studies, Figure 1.

The Apennines are an Oligocene–Quaternary fold-and-thrust belt that developed following the closure of the Mesozoic Tethys Ocean and the collision between Africa and Europe during the Alpine Orogeny (Carminati and Doglioni, 2012). Episodes of pre- and post-orogenic extension in this mountain chain have been recognized by numerous workers, (e.g. Tavarnelli, 1996a, 1996b; Tavarnelli and Peacock, 1999; Scisciani et al. 2014; Pace et al. 2014).

The Montagna dei Fiori is an overturned anticline with an NNW-SSE axial trend, which developed during the Lower Pliocene and involves the Umbria-Marche carbonate succession (Jurassic–Miocene) and the Messinian

foredeep siliciclastic deposits (Mattei, 1987; Calamita et al., 1998; Scisciani et al., 2002; Scisciani and Montefalcone, 2006; Di Francesco et al., 2010; Storti et al., 2016) (Figure 2A, B).

A regional NW-SE trending normal fault outcrops over a length of approximately 15 km in the backlimb of the anticline (Figure 2C), resulting in the tectonic contact (with a downthrow of ca 900 m) between the Jurassic–Cretaceous carbonate sequence in the footwall and the Miocene hemipelagic succession in the hanging wall.

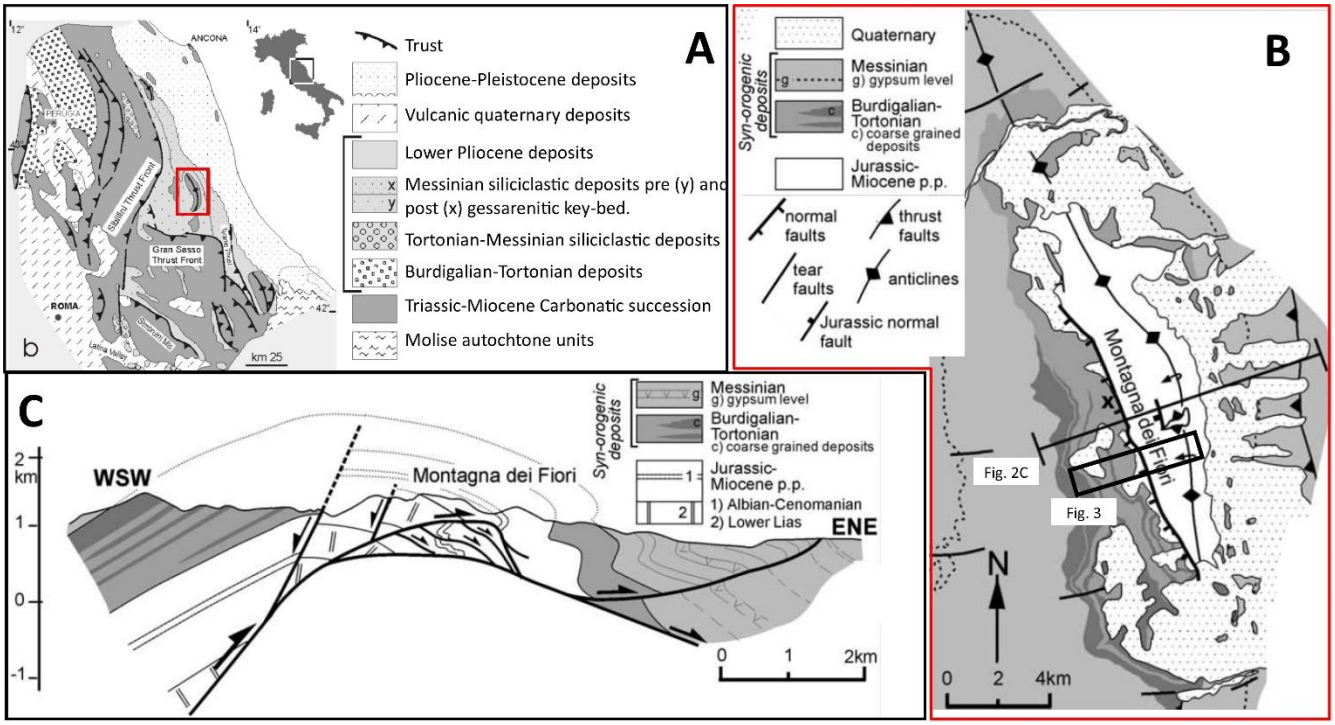

Figure 2. A) Tectonic sketch of Central Italy with the Montagna dei Fiori area highlighted by the red box B) Geological map of the Montagna dei Fiori area. C) Cross section (after Scisciani et al., 2002).

The SP52 road crosses the study area running in an E-W direction. Along the road, from West to East, the following Umbria-Marche succession formations outcrop: Marne con Cerrogna (MCERR, Miocene), Corniola Fm (COI, Early Jurassic, overlaying the older Early Jurassic Calcare Massiccio, CM), Rosso Ammonitico Fm (RAM, Early Jurassic), Formazione del Salinello and Calcari Diasprigni Fms (CDU, Late/Middle Jurassic), Maiolica Fm (MAI, Early Cretaceous), Marne a Fucoidi Fm (FUC, Early Cretaceous) and the Scaglia Rosata and Scaglia Cinerea Fms (SR, Late Cretaceous-Oligocene). Figure 3 shows the geological map (modified after Mattei, 1987) of the area (red rectangle in Figure 1) with examples of the outcrops analyzed along the SP52 road. Table 1 summarizes the characteristics of each lithology outcropping within the area.

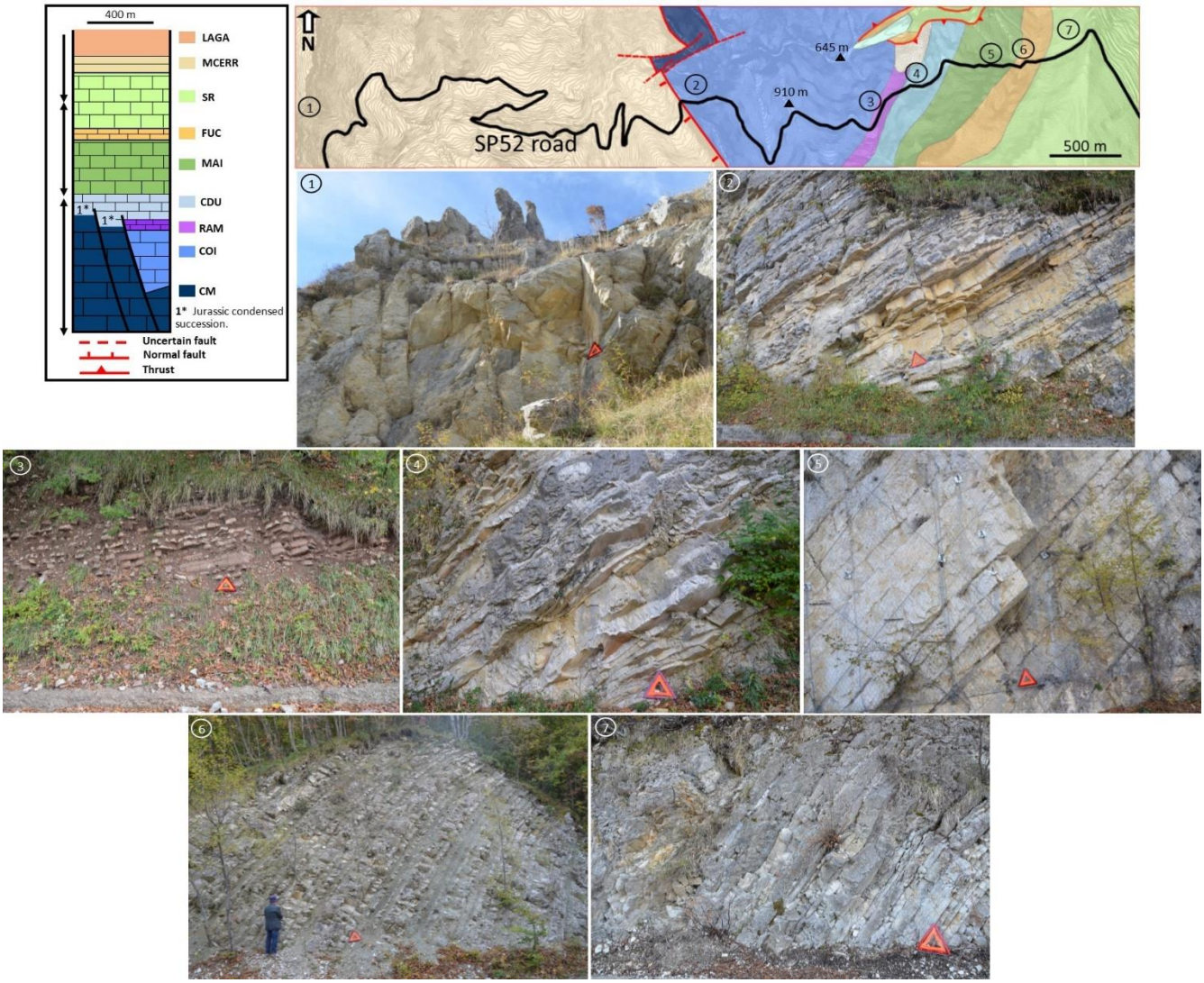

Figure 3. Geological map and stratigraphic column of the study area with photographs of outcrops 1 to 7 along the SP52 road (Black triangles in the geological map represent two reference elevation points, contour interval is 5 m). Red triangle with 0.425 cm length side as scale. 1) MCERR Formation, 2) MAI Formation, 3) RA Formation, 4) CDU Formation., 5) MAI Formation, 6) FUC Formation, 7) SR Formation. Photograph of MCERR Formation taken looking toward West, all the other photographs are taken looking toward South).

Table 1. Description of the main geological formations outcropping within the study area.

Lithology	Description
1) Marne con Cerrogna Fm. (MCERR)	Siliceous limestone, grey marls, and very thick layers of calcarenite (up to 3 m).
2) Scaglia Rosata Fm. (SR)	White and red limestone, marly limestone and clayey marls, 10-30 cm bed-thickness.
3) Marne a Fucoidi Fm. (FUC)	Gray and red marls alternating with marly limestones, 30-50 cm bed-thickness.
4) Maiolica Fm. (MAI)	White micrite limestone, beds 30-80 cm thick with grey chert nodules and lenses.
5) Formazione del Salinello and Calcari Diasprigni Fms (CDU)	Calcarenites, 30-50 cm thick beds with gray cherts and siliceous calcilutites with green cherts.
6) Rosso Ammonitico Fm. (RAM)	Red nodular limestone alternating with 10-30 cm thick red marl beds
7) Corniola Fm. (COI)	Micrite limestone and 10-80 cm thick calcarenites beds with localized dolomites.
8) Calcare Massiccio Fm. (CM)	Limestone with massive to coarse beds.

3. Methods

3.1 Structural and geomechanical field surveys

Geomechanical and structural field surveys were carried out in all the lithologies outcropping along the SP52 road. This road runs perpendicular to the Montagna dei Fiori anticline axial trend and therefore crosses most of the geological formations of the Umbria Marche succession. These formations, listed in section 2, have different lithological characteristics and it is important to understand how these differences may influence the geomechanical parameters and stability of the slopes.

A geological compass was used to measure the discontinuity orientation and a Schmidt Hammer used to estimate both the uniaxial compressive strength of the intact rocks (UCS) and the Joint Compressive Strength, JCS. A discontinuity profilometer and graduated rules were used to measure the joint roughness and joint spacing respectively. Such data were acquired along field geomechanical scanlines using different scanline orientations to decrease data orientation bias. The length of such scanlines varied in relation to the length of the outcrop from 2 m (in small outcrops) to 20 meters (in wide outcrops). Approximately 600 measurements were taken in the geological formations (at 7 main geomechanical sites, Figure 3). Using this data, geomechanical indices such as joint volumetric count ($Jv=\Sigma\ 1/S1+1/S2+1/S3$) were calculated. Furthermore, using 1 and 2 m diameter windows the discontinuity intensity (Di: including both joints and bedding) and the Joint intensity (Ji) expressed as the length of all discontinuities or joints per unit area (L-1) (Dershowitz and Herda, 1992) were calculated for each lithology. Figure 4 shows an example of a 2 m diameter window used for measurements in the FUC Fm.

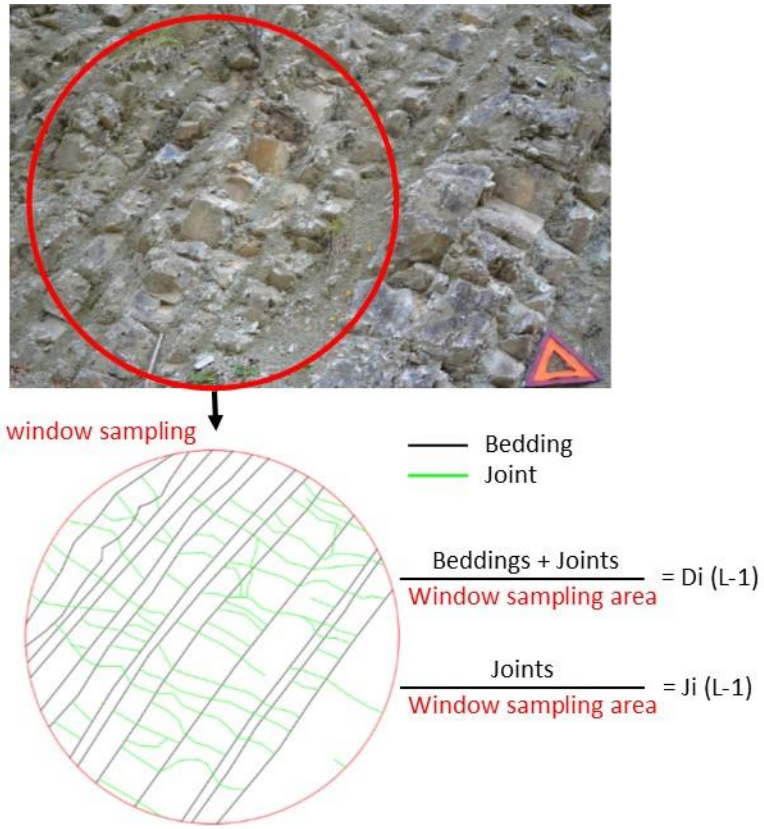

Figure 4. Example of 2 m diameter window sampling method and calculation of Di and Ji in the FUC Fm (Photograph taken looking South).

With regard to the structural geology of the area, we have analyzed the relationship between the orientation of joint sets and the structural features along the anticline. The knowledge of such relationships allowed us to understand how the joint sets vary across the anticline.

3.2 A proposed fast and low-cost photogrammetric survey method.

The use of digital photogrammetry in the study of rock slopes allows creation of 3D models, the identification of joint sets and measurement of their characteristics (such as spacing and persistence) in inaccessible and unsafe areas. Different types of photogrammetric techniques can be used in the study of rock slopes. A review of photogrammetric techniques and platforms is provided by Francioni et al. (2018c) highlighting the advantages and limitations of each system.

In this paper, we demonstrate how a fast and low-cost discontinuity survey technique can allow to rapidly and safely obtain a 3D model of the rock slopes. This approach is based on the use of a hand-held camera, so is highly suited for low-to-medium elevation rock slope investigations (Francioni et al., 2018c). A series of photographs of the outcrops are taken using different line-of-sights and the image fan method (Birch, 2006). Usually three different line-of-sights have been adopted in this study, maintaining where possible the same distance to the slope. The baseline distance between the different camera positions should be defined in relation to the distance of the camera from the slope in order to ensure the necessary overlap between photographs (suggested overlap is 80%, Agisoft, 2018). The camera used for this research is a Canon EOS 50D with a 22.3 x 14.9 mm sensor and a fixed focal lens of 20 mm. To ensure an image overlap of 80%, this requires a baseline distance between each camera station of approximately 1 m with a camera to slope distance of

approximately 3.5 m; the baseline distance is decreased as necessary when the camera to slope distance is less. The software Photoscan (Agisoft, 2018) is used to reconstruct the 3D model of the outcrops through Structure from Motion (SfM) techniques. When using SfM it is important to scale/geo-reference the model using ground control points. To avoid the use of a total station, in this study we have developed a method based on the use of a triangle of known geometry (Figure 5A, B). The triangle is located on the rock outcrops and used as reference during the photogrammetric survey (Figure 5A). A geological compass is used to measure the inclination of one of the side of the triangle and the dip direction of the triangle surface. Figure 5C shows an example of this procedure highlighting the measurements taken during the survey. Knowing the geometry of the triangle, its inclination and the dip direction of the triangle face, it is then possible to determine the coordinates of the three vertices and use them as ground control points during the subsequent 3D model construction. It is also possible to use local coordinates (where one of the vertices of the triangle is assumed to be located at 0, 0, 0) or global coordinates by measuring the location of one of the vertices with a GPS (Figure 5C). Adopting this approach, it is possible to easily create geo-referenced 3D models of the rock slope, to define the geometry of the slope (dip and dip direction) and to improve the amount of discontinuity data obtained during the geomechanical survey. Data obtained using this method have been validated against measurements taken with a geological compass during the geomechanical survey. Further geomechanical parameters such as discontinuity persistence and spacing were acquired using the same approach and integrated with data obtained during the geomechanical survey. The freeware software CloudCompare (GPL software, 2018) was utilized to manage the photogrammetric 3D model and extract all this information. Through the use of this approach it is possible to measure the orientations of fully exposed planar discontinuities, such as joint or bedding surfaces and the slope orientation. A plane is fitted to selected points on a surface (using least squares), providing an orientation estimate (dip/dip direction). Furthermore, the spacing and persistence of discontinuities can be defined by measuring the distance between two points that are manually selected in the point cloud.

An example of this procedure is shown in Figure 6, where it is possible to see the 3D model of the slope (Figure 6A), a detail of discontinuity measurements (Figure 6B), all the discontinuity attitudes taken on the slope 3D model (Figure 6C) and the definition of the slope dip and dip direction (Figure 6D).

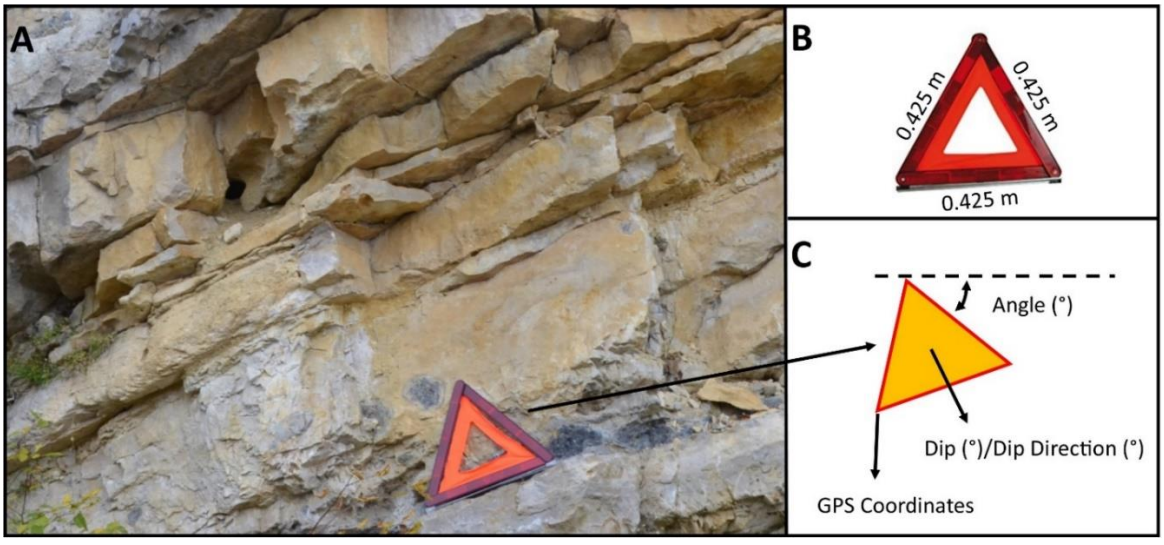

Figure 5. Use of a triangle of known size during the photogrammetric survey. A) Triangle placed on the outcrop (Photograph taken looking toward South). B) Dimension of the triangle. C) Measurements are taken of the triangle in real space to reconstruct the coordinates of the three vertices.

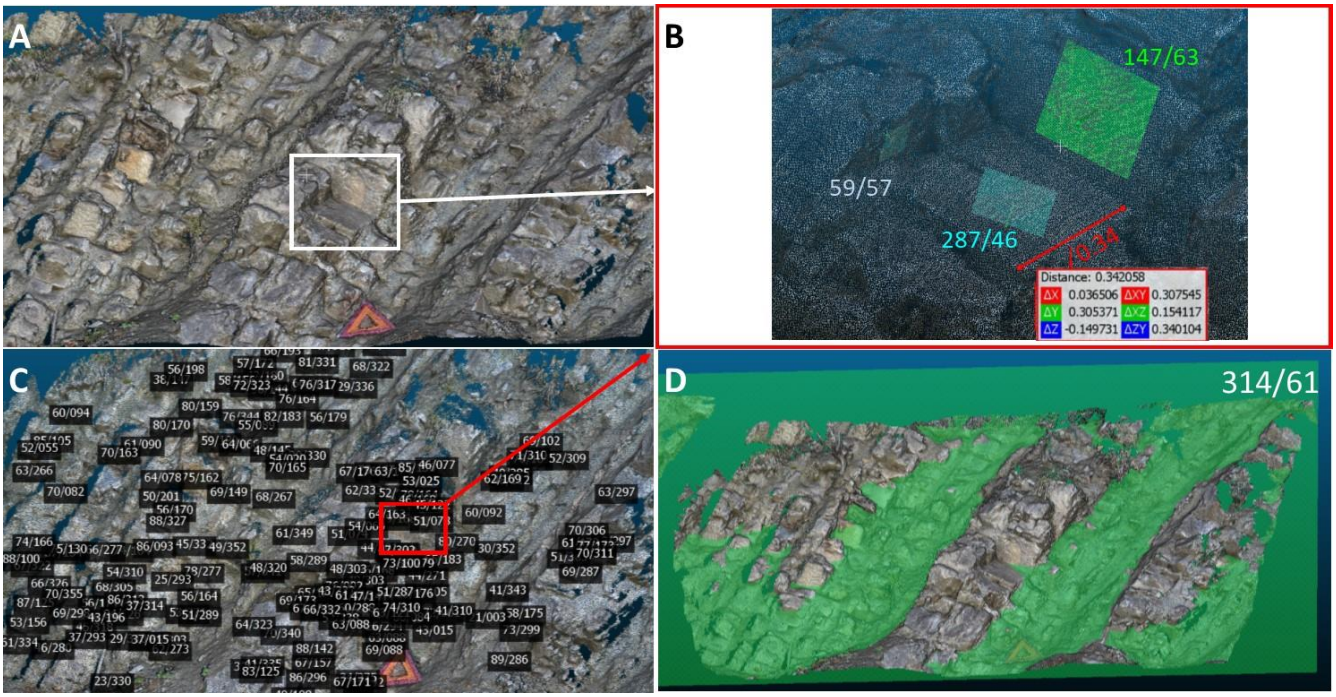

Figure 6. Example of measurements acquired in the FUC fm 3D model. A) 3D model of the slope. B) Detail of discontinuity measurements. C) Attitude of all the measured discontinuities. D) Definition of the slope dip and dip direction.

3.3 Engineering rock mass classification

Data obtained from the geomechanical and remote sensing surveys were then integrated to allow the engineering rock classification for each of the lithologies characterizing the study area and subsequently to define the rockfall risk along the SP52 road. The RMR and SMR engineering rock mass classifications were used for this purpose. The following six parameters have been used to classify the rock mass according to the RMR system: A1 - Uniaxial compressive strength of rock material; A2 - Rock Quality Designation (RQD); A3 - Spacing of discontinuities; A4 - Condition of discontinuities; A5 - Groundwater conditions; A6 - Orientation of discontinuities. The RMR can be calculated as:

RMR = RMRb + A6

where RMRb is equal to A1+A2+A3+A4+A5

A6 is defined as the rating adjustment for discontinuity orientation and changes in relation to intended engineering work (e.g. tunneling, foundation, rockfall risk map in natural slopes). However, RMR has no recommended guidelines for the definition of “rating adjustments for discontinuity orientation” for slopes and an incorrect choice of this value can overshadow and compromise any careful evaluation of the rock mass, making the engineering classification work both difficult and arbitrary (Bieniawski, 1993).

Due to this, the SMR classification through the use of the SMRTool (Riquelme et al. 2014) has been used to correct the RMRb. SMR adjusts the RMRb in relation to the orientation of joint systems and slope direction using the following formula:

SMR = RMRb + (F1 x F2 x F3)+ F4

Where:

F1 depends on angular relation between the dip direction of joints (α_j) and slope (α_s)

F2 refers to joint dip angle (β_j) for the planar mode of failure.

F3 reflects the relationship between the dip of slope (β_s) and dip of the joints (β_j).

F4 is the adjustment factor for the method of excavation and has been fixed empirically.

Table 2 illustrates the calculations proposed by Romana (1985) for defining the F1-F4 indices.

Table 2. SMR classification, after Romana et al. (2003).

ADJUSTING FACTORS FOR JOINTS (F_1, F_2, F_3)	*αj = DIP DIRECTION OF JOINT* *βj = DIP OF JOINT* *αs = DIP DIRECTION OF SLOPE* *βs = DIP OF SLOPE*				
	VERY FAVOURABLE	*FAVOURABLE*	*FAIR*	*UNFAVOURABLE*	*VERY UNFAVOURABLE*
PLANE FAILURE $\lvert\alpha j-\alpha s\rvert$ = *TOPPLING* $\lvert\alpha j-\alpha s-180°\rvert$ =	*> 30°*	*30° - 20°*	*20° - 10°*	*10° - 5°*	*< 5°*
F_1 VALUE	*0.15*	*0.40*	*0.70*	*0.85*	*1.00*
RELATIONSHIP	**$F_1 = (1 - \sin \lvert\alpha_j-\alpha_s\rvert)^2$**				
$\lvert\beta j\rvert$ =	*< 20 °*	*20°-30°*	*30°-35°*	*35°-45°*	*>45°*
F_2 VALUE *PLANE FAILURE*	*0.15*	*0.40*	*0.70*	*0.85*	*1.00*
TOPPLING	*1.00*				
RELATIONSHIP	**$F_2 = tg^2 \beta j$**				
PLANE FAILURE $\beta j-\beta s$ =	*>10°*	*10°-0°*	*0°*	*0°-(-10°)*	*<(-10°)*
TOPPLING $\beta j+\beta s$ =	*< 110°*	*110°-120°*	*>120°*	*-*	*-*
F_3 VALUE	*0*	*-6*	*-25*	*-50*	*-60*
RELATIONSHIP	**F_3 (BIENIAWSKI ADJUSTMENT RATINGS FOR JOINTS ORIENTATION, 1976)**				
F_4 ADJUSTING FACTOR FOR EXCAVATION METHOD	**F_4 = EMPIRICAL VALUES FOR METHOD OF EXCAVATION**				
	NATURAL SLOPE	*PRESPLITTING*	*SMOOTH BLASTING*	*BLASTING or MECHANICAL*	*DEFICIENT BLASTING*
F_4 VALUE	*+15*	*+10*	*+8*	*0*	*-8*

Using the SMRTool it is also possible to calculate the line of intersection between joint sets and consider the possibility of wedge failures. It is important to consider that the SMR values change within the same geological formation in relation to the road/slope orientation. In this context, we have used GIS methods to define slope dip and dip direction in areas where photogrammetric 3D slope models were not available and to calculate the SMR in the different road sections.

Romana (1985) proposed five different rock classes: Class I (SMR<20), Class II (20<SMR<40), Class III (40<SMR<60), Class IV (60<SMR<80), Class V (80<SMR<100) and in relation to these, the most appropriate mitigation works (Romana, 1993). Nevertheless, as noted by Romana (1993), it is important to remember that "the study of potentially unstable rock slopes is a difficult task requiring careful field work, detailed analysis and good engineering sense in order to understand the relative importance of the several instability factors acting on the slope". In fact, in sedimentary and heterogeneous successions such as found in the Umbria-Marche area, it often occurs that different geological formations present similar SMR values. This is for example the case for the calcarenite layers of the MCERR Formation and the FUC or RA formations. The calcarenite layers of the MCERR Formation (Figure 7A) are characterized by the sporadic failures of very large blocks while the FUC and RA formations (Figure 7B for FUC) by more systematic failures of small blocks. To overcome this problem, Romana (1993) suggested the use of the joint volumetric count, Jv, to facilitate the choice of the most appropriate mitigation works.

However, when considering lithotypes characterized by the alternation of limestone and marls such as the RA and FUC formations, the Jv alone is not sufficient to understand the behavior of the rock mass, which is

strongly influenced by the interaction of the marls/limestone layers and the orientation of the bedding planes. In fact, in such geological formations, it is possible to have both low volume block failures (related to the interaction between joint sets and beds and controlled by the typical thin limestone layers of such formations) or, when the appropriate kinematic condition exists, very large slope failures along the marl/bedding planes. The identification of these two possible types of failures can be related to the location of the slope within the anticline and to the dip direction of the slope/road cut. Figure 8A shows a conceptual model of an anticline highlighting this feature. When the strike of slope/road cut is perpendicular to the strike of the anticline axial plane, the bedding planes/marl layers will be sub-horizontal or will strike perpendicular to the slope (Figure 8A, B and C). In such conditions the failure of low volume blocks is to be expected. In contrast, when the strike of slope/road cut dip is parallel to the fold axial surface direction, the bedding planes/marls layers will dip in the same direction as the slope increasing the possibility of large slope failure occurrence (Figure 8A and D) (Badger, 2002; Stead and Wolter, 2015).

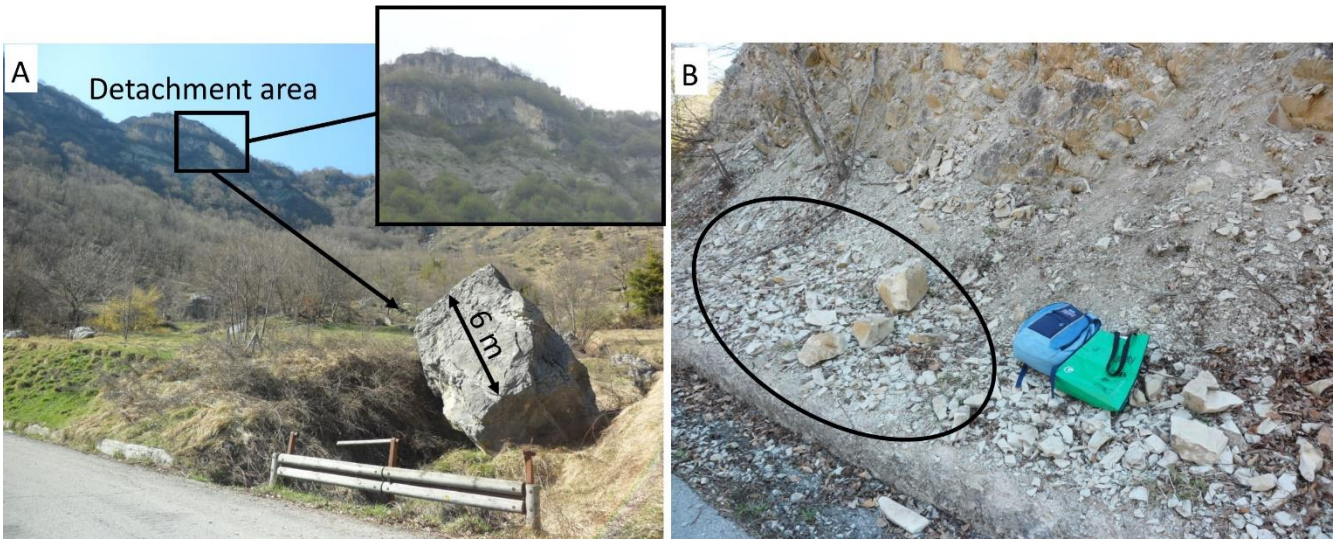

Figure 7. A) Large block failed from MCERR Formation. B) Small blocks failed from FUC Formation.

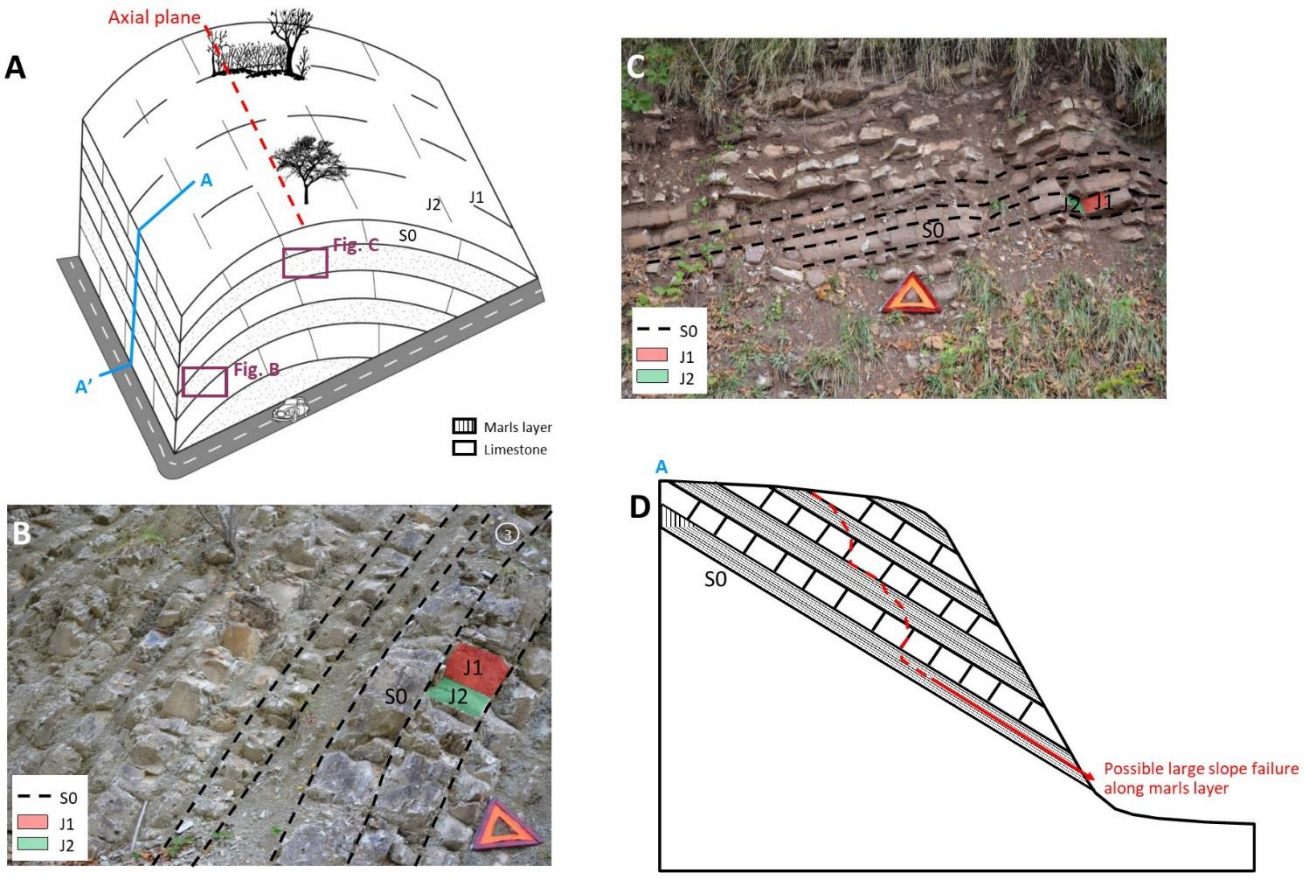

Figure 8. A) Conceptual model showing the importance of slope location within an anticline. B) Small blocks failing from FUC Formation due to the interaction of joint sets and transverse S0 joints. C) Small blocks failing from RA Formation due to the interaction of joint sets and sub-horizontal S0. D) Conceptual model of possible slope failure related to unfavourable kinematic conditions (S0 daylighting in the slope).

In this context, it is clear that such geological formations (i.e. FUC and RA in the study area) should be treated differently in relation to the local kinematic conditions. We suggest a new approach based on the use of the slope/discontinuity angular relationship parameters F1, F2 and F3 (related to the bedding S0) of the SMR classification (Figure 7). These parameters control the kinematic relationship between the rock slope and the discontinuities and therefore provide important information on the possibility of failure. When dealing with heterogeneous rock masses characterized by the alternation of marls and limestone, the bedding planes, S0, will have the same orientation as the impermeable marl layers. Therefore, when analyzing the parameters F1, F2 and F3 related to the bedding S0, it is possible to identify whether failures such as those highlighted in Figure 8D may occur. In particular, this would be possible where the bedding planes (and consequently the marl layers) have a dip direction similar to the slope dip direction, with a dip greater than 30° (assumed friction angle for the marl layer, derived from previous research and consulting works carried out in similar formations within the Umbria-Marche Apennines, e.g. Regione Marche, 2002; Cencetti and Conversini, 2003) and lower than the slope dip. This can be summarized using the F1, F2 and F3 parameters as:

- $F1 \geq 0.4$ ($|\alpha_j - \alpha_s| < 30°$)
- $F2 \geq 0.7$ ($\beta_j \geq 30°$)
- $F3 \leq -50$ ($\beta_j - \beta_s < 0°$)

If the three conditions above are fulfilled, the potential instability could be in the form of a large slope failure (e.g. Figure 8D) and the mitigation work proposed by Romana should be modified (restyling/re-excavation should be considered). In all the other cases, the volume of potential rockfall can be related to the Jv and the Romana (1993) guidelines consulted.

3.4 GIS analysis

To develop the rockfall risk map for the SP52 road based on the calculated SMR classes and to improve the calculation of SMR values, a GIS platform was used to store all the data obtained during the geomechanical and photogrammetric surveys.

The geological map of the area has been digitized in ESRI ArcMAP (ESRI, 2018) (Figures 3 and 7). Information gained from the geomechanical analysis and RMR analysis, such as joint sets, Jv, Di, Ji and RMRb were included in the GIS database. Furthermore, through use of spatial analysis techniques, the linear feature demarcating the SP52 road has been sub-divided in relation to both the geological formations characterizing each section of the road and to the estimated SMR classes.

The dip and dip direction of the slopes above the SP52 road have been extracted from the photogrammetric 3D model (Figure 6) and, when this was not available, through the GIS Slope and Aspect thematic maps generated using a 10 m resolution Digital Elevation Model available through the Abruzzi Region open data (2018).

The integration of this GIS spatial analysis technique with the geological, structural geological and geomechanical information allows calculation of the SMR for each section of the road.

4. Results

4.1 Rock mass analyses through geomechanical, structural and remote sensing surveys

During the field geomechanical survey 630 measurements were taken including 200 bedding plane and 430 joint dip/dip direction measurements. The analysis of this data showed the bedding planes to have a N-S strike with a dip toward the West in the backlimb of the anticline and toward the East in the forelimb (Figure 9). Figure 9 shows the geological map of the area, the cross section along A-A’ and stereoplots of the bedding plane attitudes from field surveys.

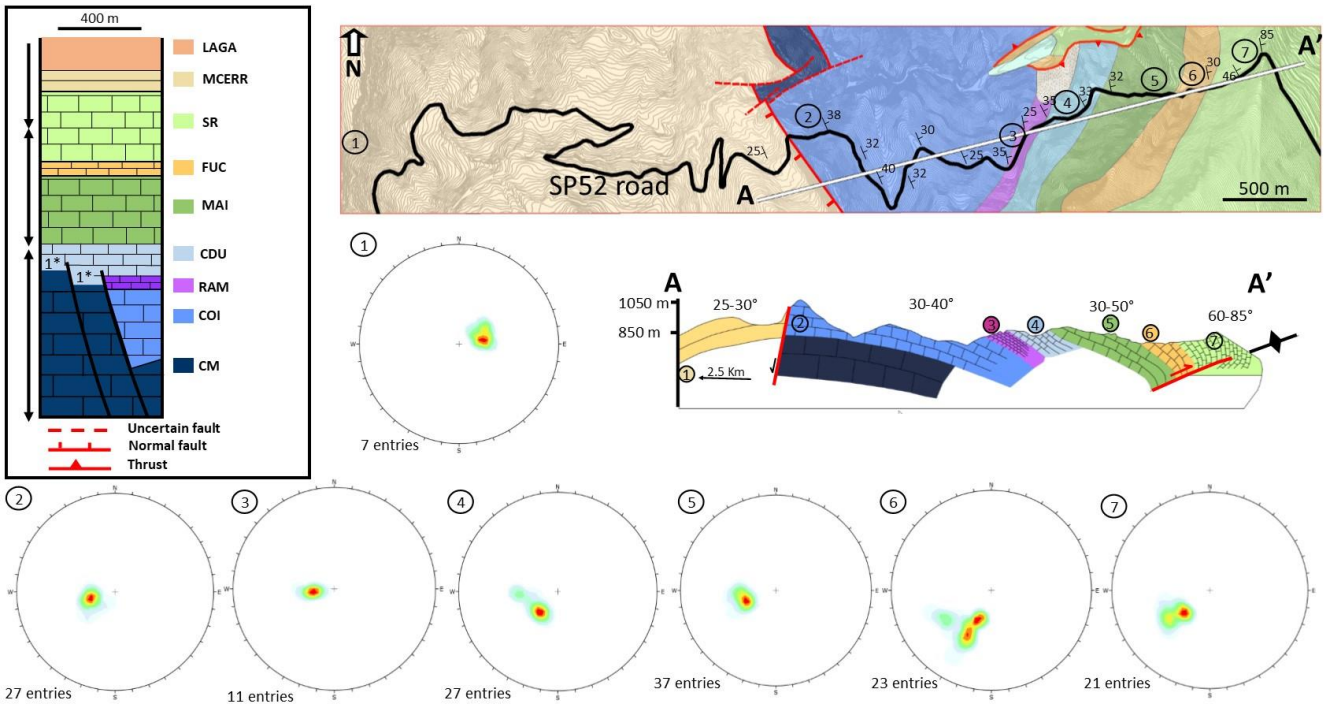

Figure 9. Geological map of the area and the A-A' cross section with the bedding plane stereoplots from field surveys (contoured pole vector data using lower hemisphere, equal area projection) .

With regard to the joint sets, the anticline is characterized by two main joint sets, J1 (sub-vertical and approximately ENE-WSW oriented) and J2 (approximately N-S oriented), transversal and longitudinal to the fold axial trend respectively. Figure 10A shows the stereoplots representing the joints and bedding planes from the geomechanical field survey. The transversal joint set J1 is the dominant set (with higher persistence) with J2 terminating against it forming a T-shape joint termination. J1 and J2 are always orthogonal to the bedding planes within the anticline and are interpreted as extensional joint sets (Price et al., 1966; Watkins et al., 2017).

The photogrammetric survey allowed creation of a 3D model of each outcrop and significantly increased the amount of data collected from the field geomechanical survey. Figure 10B shows stereoplots of discontinuities measured from the photogrammetric point clouds. Figure 10C shows the stereonet obtained from the integration of field geomechanical and remote sensing data while Figure 11 illustrates the 3D models of the outcrops obtained with the proposed photogrammetric approach.

The similarity between the field geomechanical survey and the photogrammetric stereoplots (Figure 10A and B) clearly demonstrates the validity of the proposed photogrammetric approach. Moreover, a further validation was carried out comparing conventional field mapping and photogrammetric measurements. Figure 12 shows an example of this procedure in the FUC Formation (Figure 12A), highlighting the close agreement between conventional field mapping measurements (Figure 12B) and photogrammetric data (Figure 12C).

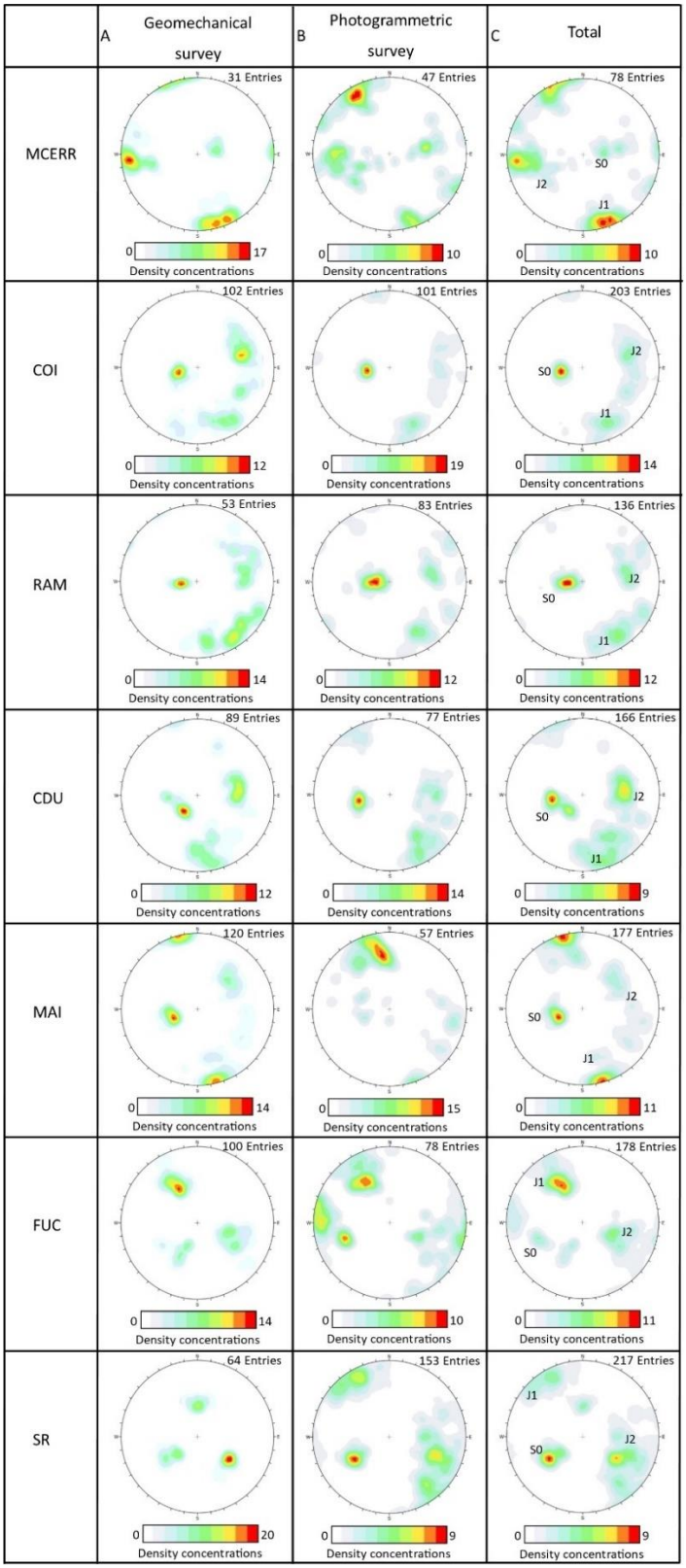

Figure 10. Stereonets created using conventional field-based geomechanical scanlines (A), photogrammetric 3D models (B) and the integration of both data sets (C). Plot mode: contoured pole vectors, equal area, lower hemisphere.

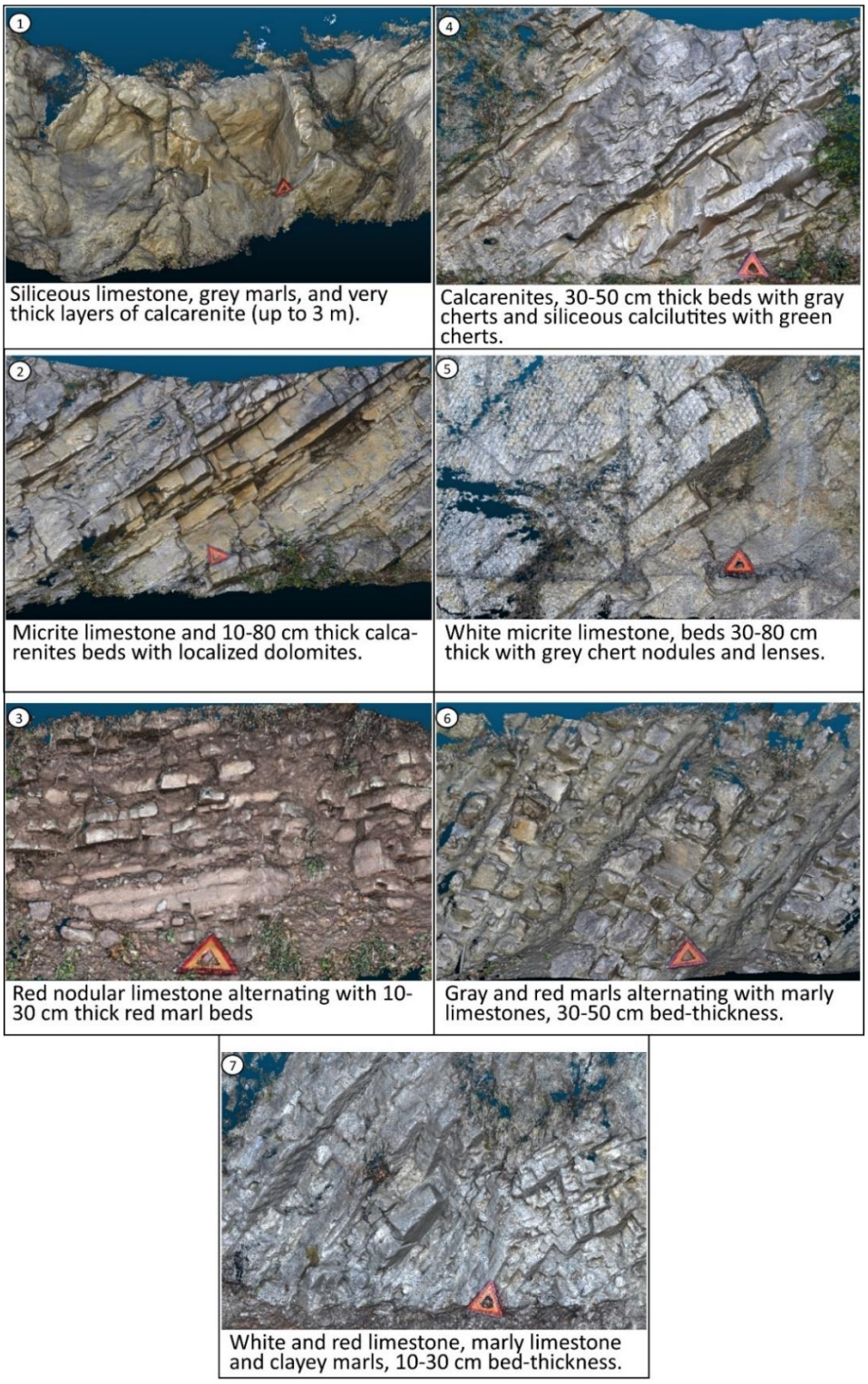

Figure 11. 3D models of the outcrops along the SP52 road. 1) MCERR Formation. 2) COI Formation. 3) RA Formation. 4) CDU Formation. 5) MAI Formation. 6) FUC Formation. 7) SR Formation. Photographs of MCERR taken looking toward West, all the other photographs taken looking toward South.

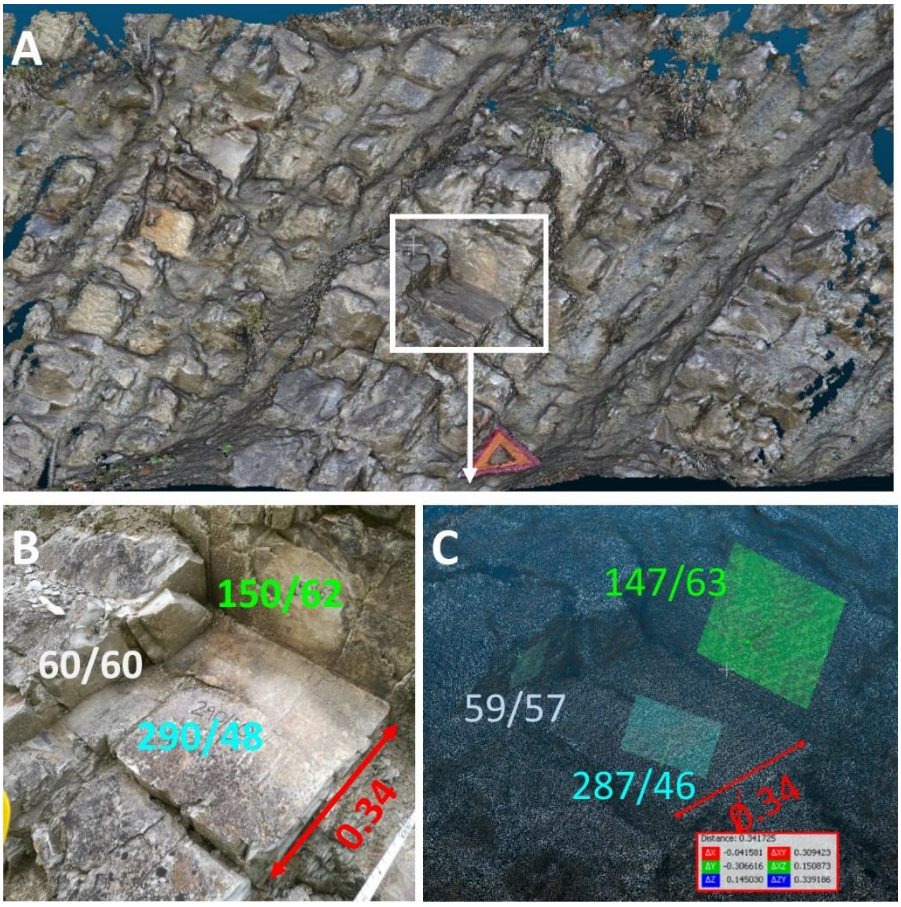

Figure 12. FUC Formation (A) and validation of the proposed photogrammetric approach through the comparison of field geomechanical survey (B) and photogrammetric measurements (C). Differences are consistently within 5°.

Tables 3 and 4 highlight the main joint sets and the geomechanical characteristics/indices of each geological formation respectively. Table 5 shows the Di and Ji obtained from 1 and 2 m diameter window sampling.

Data presented in Tables 3 to 5 are strongly influenced by the geological and structural characteristics. In particular, formations characterized by thin limestone beds (10-30 cm thick) or limestone alternating with marls (such as the RA and FUC formations) present higher values of Jv (Jv=26 and 14.2 respectively) and joint intensity (Ji=5.2 and 6.5 m-1 respectively). In more homogeneous formations, such as the COI, MAI and the calcarenite layers of the MCERR formations (micrite limestone or calcarenites with thick beds from 0.3 to 3 m thick) we obtained lower Jv (9.2, 12.1 and 1.2 respectively) and Ji values (4, 3.7 and 3.8 respectively). Aperture of fractures in some outcrops (such as in the case of CDU, COI and MAI formations) show a wide range (Table 4), probably related to the method of road excavation (mechanical and/or blasting).

Table 3. Dip and dip direction of the main joint sets (degrees) with number of poles and Fisher K values for each formation.

Formation	Joint set	Dip°/Dip Dir°	n. poles	Fisher K
SR	S0	51/058	50	42
	J1	89/140	42	26
	J2	58/293	63	24
FUC	S0	50/42	30	17
	J1	63/151	63	30
	J2	61/291	72	12
MAI	S0	39/077	45	44
	J1	86/163	67	16
	J2	59/243	44	12
CDU	S0	36/066	45	28
	J1	54/264	59	15
	J2	74/336	48	28
RA	S0	22/088	48	37
	J1	78/324	42	16
	J2	66/249	40	17
COI	S0	31/077	58	51
	J1	77/339	47	28
	J2	69/256	59	22
MCERR	S0	41/255	16	18
	J1	89/337	27	23
	J2	69/083	31	14

Table 4. Geomechanical characteristics of geological formations (discontinuity properties refer to the most critical joint sets in each formation).

Formation	UCS (MPa)	RQD%	Spacing (m)	Length (m)	Aperture (mm)	Roughness	Infilling	Weathering	Jv
SR	67	61	0.18	15	1-5	Rough	soft	moderate	12.5
FUC	64	68	0.18	15	1-5	Smooth	soft	moderate	11.5
MAI	75	75	0.23	15	2-30	Smooth	soft	moderate	8.9
CDU	74	57	0.11	20	1-100	Rough	soft	moderate	17.9
RA	59	29	0.1	15	1-7	Rough	soft	high	23.5
COI	85	81	0.3	10	1-100	Rough	soft	high	6.7
MCERR	46	99	1	20	2-20	Rough	soft	moderate	2.4

Table 5. Di and Ji obtained from 1 and 2 m diameter window sampling.

Formation	Di (m^{-1})	Ji (m^{-1})
SR	12.7	4.2
FUC	13.8	6.5
MAI	6.8	3.7
CDU	9.1	3.9
RA	13.6	5.2
COI	9	4
MCERR	5	3.8

4.2 RMR and SMR rock mass classifications

Data obtained from the field geomechanical and photogrammetric surveys have been used to classify the rock masses according to the RMR and SMR engineering rock mass classifications. Table 6 shows the RMRb obtained from the sum of A1, A2, A3, A4 and A5.

Table 6. Estimated RMR parameters and calculated RMRb values for each formation.

Formation	A1	A2	A3	A4	A5	RMRb
SB	7	13	10	13	15	58
FUC	7	13	10	9	15	54
MAI	7	17	10	7	15	56
CDU	7	13	8	11	15	54
RA	7	8	8	9	15	47
COI	7	17	10	10	15	59
MCERR	4	20	20	10	15	69

The RMRb values, together with the geomechanical indices and 3D models were stored in a GIS database.

Furthermore, using GIS spatial analysis techniques the SP52 road was divided according to the geological formations outcropping (Figure 13A and B) in order to visualize the geomechanical information for each rock slope above the road. Figure 13C shows an example of this procedure for the FUC formation.

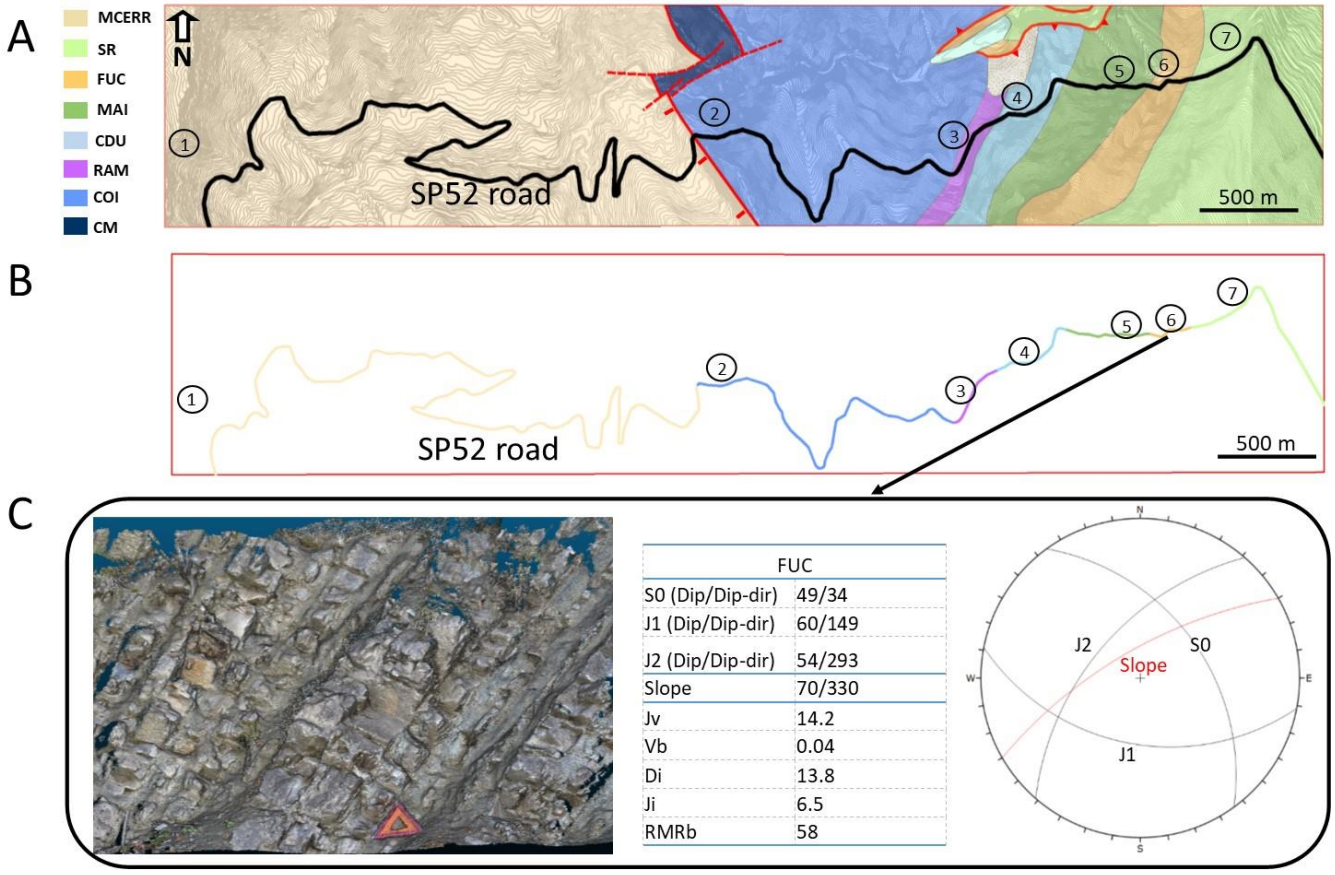

Figure 13. A) Geological map and route of the SP52 road. B) Sub-division of the SP52 road according to the geological formation. C) Example of GIS database for section (6) of the road in the FUC Formation.

As previously mentioned, the SMR classification has been used to classify the rock masses along the road. The SMR adjusts the RMRb in relation to the orientation of joint systems and slope attitude. In the case of sub-vertical joint set, such as J1 (with poles dipping both toward NNW and SSE, Figure 10), the SMR was calculated considering both possible dip directions.

Where the photogrammetric 3D model of the slope was not available, the slope dip and dip direction were calculated using the GIS Slope and Aspect maps (Figure 14) extracted from a 10x10 m resolution DEM (see section 3.4).

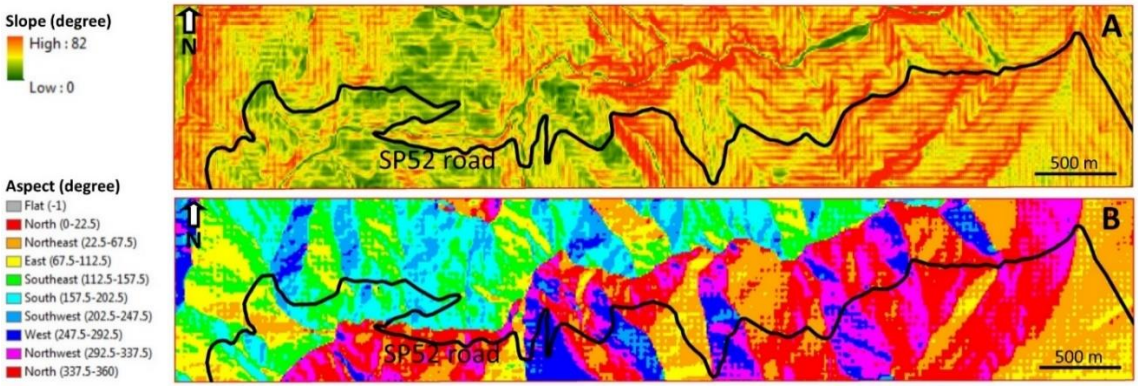

Figure 14. GIS Slope (A) and Aspect (B) thematic maps.

The information obtained from the GIS thematic maps (slope dip and dip direction) was integrated with data obtained from previous photogrammetric, field geomechanical and GIS analyses to calculated the SMR for the different road sections. An example of such an analysis is shown in Figure 15A-C, highlighting an example (red rectangle) of how it is possible to calculate the SMR using the information stored within the GIS database.

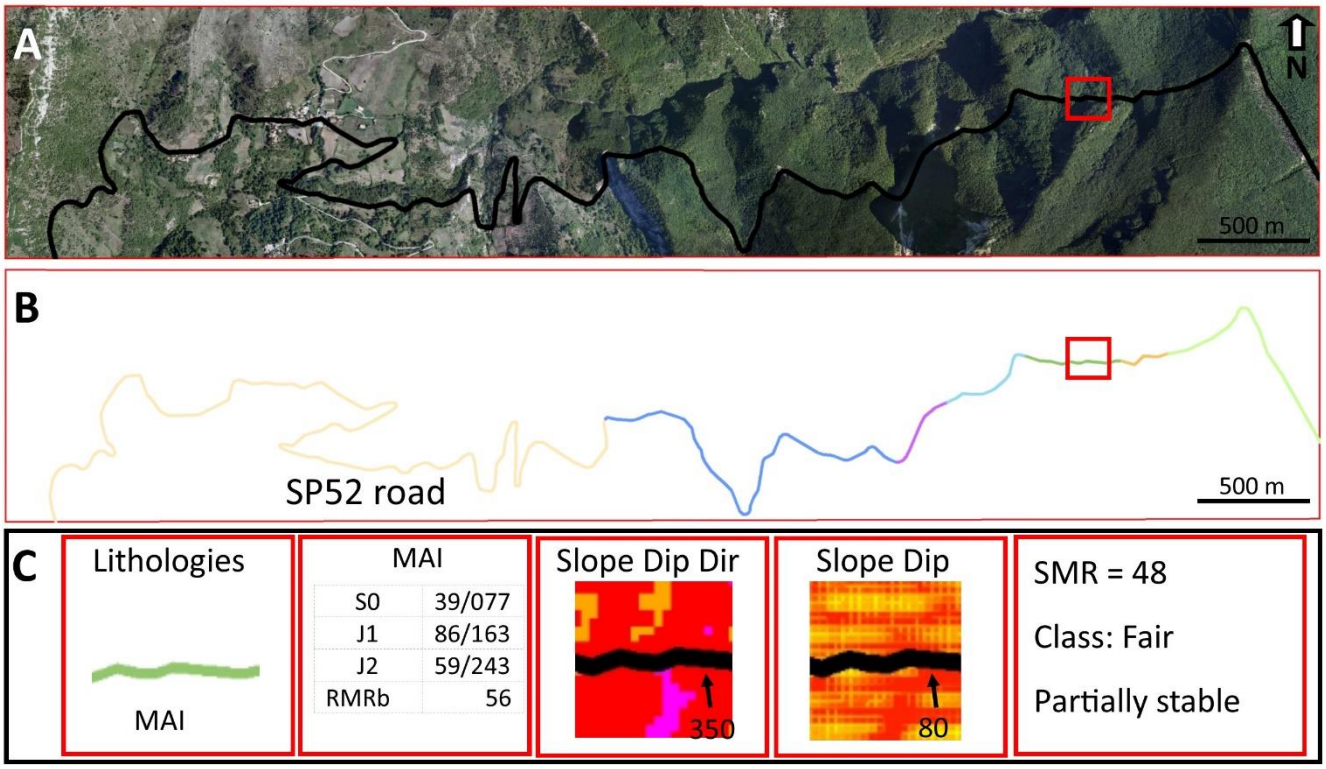

Figure 15. Example of SMR calculation. A) Orthophoto with highlighted section of the SP52 road. B) Definition of the lithology for the road section highlighted in A (MAI Formation.). C) Procedure and data used for the calculation of SMR.

The estimated SMR values were subsequently associated to the different road sections (Figure 16A, B). Figure 16C highlights the classes proposed by Romana in relation to the calculated SMR values. Because the calculated SMR values are influenced by slope attitude, it is possible to obtain varied SMR values within the same geological formation (Figure 16B).

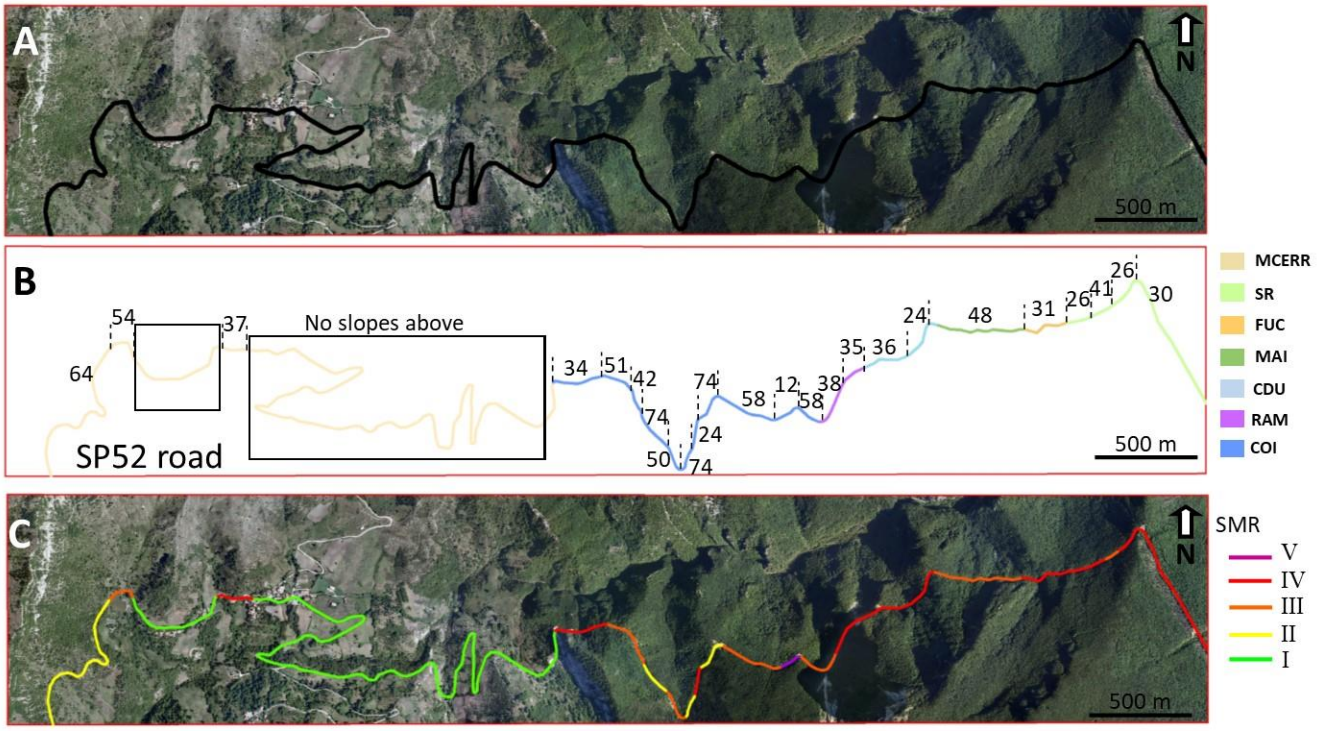

Figure 16. SP52 road (A) and associated SMR values (B) and SMR classes (C). Black rectangles represent zones with no slopes above the road.

4.3 A proposed modification of SMR estimation for heterogeneous rocks.

Romana (1993) suggests the combined use of SMR and Jv for the definition of the most appropriate rock slope mitigation works. However, as discussed previously, in heterogeneous rock masses the use of Jv may not be adequate and for this reason we have included in the GIS database the F1, F2 and F3 parameters. Figure 17A shows the Jv corresponding to each of the geological formations along the SP52 road while Figure 17B provides a map with the highlighted SMR classes, Jv values (white numbers) and, in the case of heterogeneous rocks (i.e. MCERR and RA), the F1, F2 and F3 parameters (light-blue numbers). When the F1, F2 and F3 parameters are not present, the SMR class and the Jv should be used according to Romana (1993) to suggest the most appropriate mitigation work. When in heterogeneous rocks the three conditions ($F1 \geq 0.4$, $F2 \geq 0.7$ and $F3 \leq -50$) are fulfilled, a slope modification is suggested. In this case example, none of the heterogeneous rocks (MCERR and RA) needs mitigation or regrading.

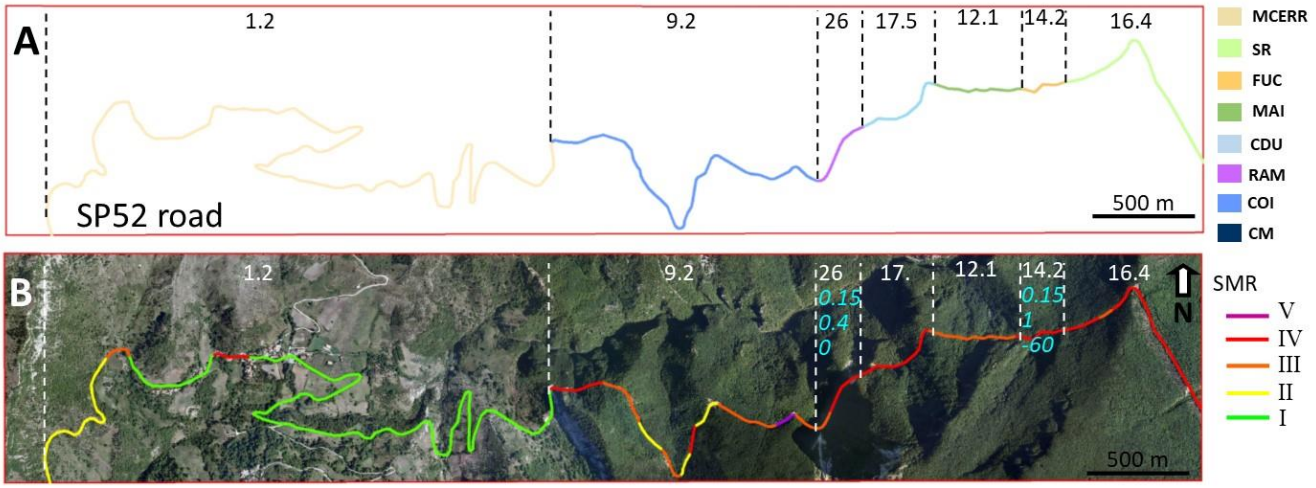

Figure 17. A) Jv values (black numbers) corresponding to each geological formation. B) Jv values (white numbers) corresponding to the SMR classes, light blue numbers represent F1, F2 and F3 values in heterogeneous rock masses (FUC and RA).

4.4 Proposed mitigation works

According to Romana (1993) and the proposed approach (GIS-geomechanical-remote sensing with SMR classes and the F1, F2 and F3 parameters) the most appropriate mitigation works relative to all the geological formations outcropping in the study area can be suggested:

- SR Formation presents SMR ranging from class II to class IV. Due to the high degree of fracturing and the elevated Jv (Jv = 16.4), slope rockfall ditches are suggested for road sections with SMR II (dimension of the ditch can be defined in relation to the slope height (Romana, 1993). For SMR III, the use of rockfall nets would be recommended. In case of SMR IV, rockfall nets could be integrated with toe walls where necessary. Systematic bolting at 1 m distance combined with a continuous thick layer of shotcrete could be a further solution for SMR class IV. However, due to environmental factors and the importance of tourism in the area and the consequent high impact of shotcrete on the aesthetics of the landscape, this solution should be avoided. Although more expensive, a road shed could be an alternate solution for SMR IV.

- FUC Formation falls into SMR class IV. The three conditions (F1 ≥ 0.4, F2 ≥ 0.7 and F3 ≤ -50) for slope failure are not fulfilled (F1 < 0.4) and for this reason Romana's guideline (1993) and Jv are used to suggest the most appropriate mitigation works. Due to the elevated Jv (Jv = 14.2), large slope ditches or toe walls and rockfall nets are suggested.

- MAI Formation is classified as SMR III. Considering Jv = 9, reinforced nets and systematic bolting at 1-3 m distances (three times the prevalent joint spacing) is suggested.

- CDU Formation is classified as SMR class IV. Due to the elevated degree of risk and Jv (Jv = 17), the use of nets and toe walls is suggested. For the same reasons explained in the case of SR, systematic bolting at 1 m distance combined with a continuous thick layer of shotcrete could be a further solution but should be avoided. A road shed could be an alternate solution.

- RA Formation has an SMR ranging from class III to VI and Jv = 26, F1 = 0.15, F2 = 0.4, F3 = 0. The three conditions (F1 ≥ 0.4, F2 ≥ 0.7 and F3 ≤ -50) for rock slope failure are not fulfilled and for this reason Romana (1993) and Jv are used to suggest the most appropriate mitigation works. Due to the elevated Jv, for SMR Class VI large slope ditches or toe walls and nets are suggested. In the case of class III, slope ditches and/or and nets are proposed.

- COI Formation has an SMR ranging from class II to V. Considering Jv = 9.2, reinforced nets and systematic bolting at 1-3 m distances (three times the prevalent joint spacing) are suggested together with toe wall or road sheds. In the case of SMR class II, nets or large slope ditches are proposed.

- MCERR Formation has an SMR ranging from class II to III. Considering Jv = 1.2, bolting at 3-3.5 m distances or anchors are suggested. When the installation of these mitigation works is not possible, the installation of rock fall barriers with high energy absorption capacity may be suggested.

5. Discussion

The choice of a specific rock mass classification is an important step in engineering projects. Most rock mass classification systems have been developed for mining engineering or underground excavation and their use in natural slopes or heterogeneous rocks is often challenging (Romana 1993). Among the most used systems, the RMR, the Q system and the recently developed Q slope system were developed specifically for mining and civil engineering respectively. The SMR and the GSI are common methods used for characterizing natural slopes or road cuts. The SMR includes suggestions on possible mitigation works but, in the case of heterogeneous rock masses, the possible role of impermeable layers on the overall slope stability has not been considered. The GSI was specifically developed to provide parameters for numerical modelling of rock masses and can be easily used in the case of heterogeneous rocks (Marinos and Hoek, 2001) but was not designed to provide information on support and mitigation works in natural slopes. Marinos (2012) has analyzed different types of tunnel behavior in relation to the type of rock/ geology and, using the results of such research, suggested the most appropriate tunneling support measures; the use of GSI in support recommendations however is still very limited compared to Q and RMR.

The geology and the structural geology of an area can play an important role in the choice of the most appropriate classification system, both in tunneling and slope analyses. In this research, we highlight how the thickness and the attitude of the bedding planes and the heterogeneities within the rock mass must be considered in the analysis of rock slopes. The bedding plane spacing/bed thickness plays an important control on the geomechanical characteristics of a rock mass (McGinnis et al., 2017; Watkins et al., 2017) influencing Di, Ji and Jv values and, consequently, the most appropriate mitigation methods (Romana, 1993). Furthermore, geological formations characterized by alternation of limestone and impermeable layers could generate large scale slope failures when the appropriate kinematic conditions exist. In this research we propose the use of the slope-discontinuity angular relation parameters F1, F2 and F3 to verify the possibility of such large failures in heterogeneous rocks. We suggest the use of F2 ≥ 0.7 ($\beta j \geq 30°$) assuming 30° of friction angle for marls layers in the presented case study; this parameter should be modified as appropriate for different lithologies.

To improve the geological and geomechanical information we have used digital photogrammetry. The use of such remote sensing techniques has been extensively documented in the last two decades (Sturzenegger and Stead, 2009; Salvini et al., 2013; Francioni et al., 2015; Wolter et al., 2016; Donati et al., 2017). In this research, to overcome problems related to the scaling and georeferencing of photogrammetric models, we introduce a

new approach which allows the rapid and low-costs creation of georeferenced rock slope point clouds. The method is based on the simple use of a digital camera and a geological compass without the need of a total station for scaling and georeferencing the models. Avoiding the use of the total station makes the proposed method easy to apply and, more importantly, the survey is faster reducing the risk for the surveyor and the cost of the field work/hardware. With regard to the software necessary for data post processing, the costs are the same as for conventional photogrammetric techniques, with the possibility to use open source software, e.g. VisualSFM (Wu, 2011) for Structure from Motion and CloudCompare (GPL Software, 2018) for managing the point clouds, in addition to proprietary software, such as Agisoft Photoscan (Agisoft, 2018). The use of this method has been demonstrated for slopes up to 5 meters high; its reliability for higher slopes is based on the dimension of the object of known geometry used for scaling the model. For this reason, the proposed method is therefore recommended for outcrops less than 5 meters high and suggested with the use of total station for higher slopes. The good agreement between conventional field mapping and photogrammetric measurements demonstrates the validity of the proposed photogrammetric approach. However, comparing the stereoplots obtained from the two techniques, there tends to be slightly more scatter in the photogrammetric survey data compared to the conventional field mapping data with minor differences in recorded strike. This may be related to the fact the field geomechanical surveys are undertaken in smaller accessible areas of the slopes while the photogrammetric model allows measurements to be made over wider areas and hence is characterized by higher joint set variability.

In the proposed methodology the main joint set orientations and their variability within the outcrop itself, plays an important role. An example is shown in Figure 18, which illustrates the dip/dip direction variation of the J1 system within a 3D model of the COI Formation. This variation, clearly visible in the photogrammetric 3D model, was not detected during the field geomechanical survey due to the elevation of the outcrop. The SMR analysis of J1 using these two possible dip directions (NNE and SSW) highlighted potential toppling failure, otherwise unidentified from conventional field survey data alone. In this context, it is important to undertake the SMR classification using a statistical analysis of joint set orientations and, if possible, to improve the conventional field mapping dataset wherever possible with data from remote sensing surveys.

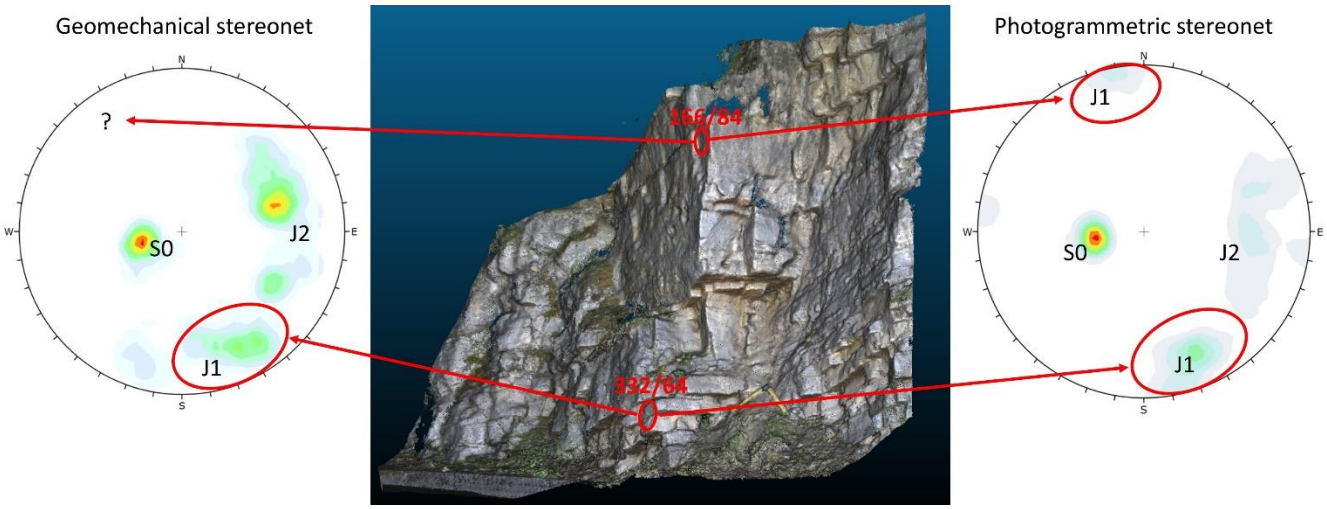

Figure 18. 3D model of the COI Formation outcrop showing the variation in the dip of J1. This variation, visible in the photogrammetric stereoplot, was not detected in the field geomechanical survey.

The conventional field geomechanical and photogrammetric data have been managed through the use of GIS. The use of this technique in the study of slopes has been documented by many authors including Van Westen

(1998), Xie et al. (2006), Yilmaz et al. (2012), Audisio et al. (2017) and Francioni et al., (2018a and 2018b). In this paper we propose a semi-automatic procedure which allowed the convenient and rapid calculation of the SMR along the SP52 road. The final map shown in section 4.3 represents the SMR values obtained, the Jv, and the F1, F2 and F3 parameters. This map represents an extremely useful tool that can be used to easily define the most appropriate mitigation works in relation to the suggested guidelines of Romana (1993). A new SMR methodology for recommending mitigation works in heterogeneous rock masses is proposed in this research. The methodology is based on the integrated use of conventional and photogrammetric surveys, in the definition of F1, F2 and F3 parameters and the analysis of lithotypes. Figure 19 shows a flow chart that summarizes step by step the proposed methodology. As emphasized by Romana (1993) it is important to note that the study of potentially unstable rock slopes and the most appropriate support methods is a difficult task requiring careful field work, detailed analysis and good engineering sense in order to understand the relative importance of the several instability factors acting on the slope.

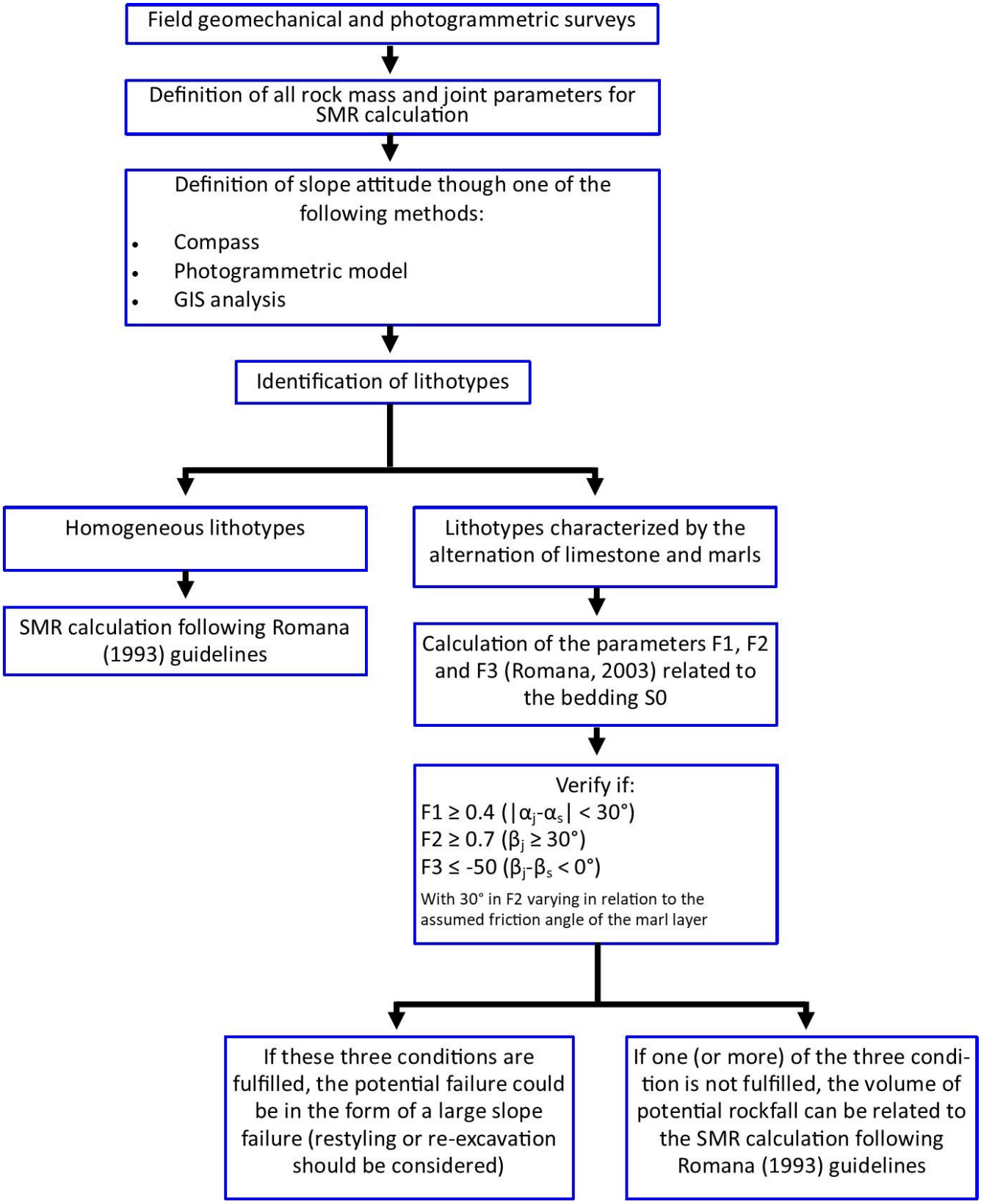

Figure 19. Flowchart illustrating the steps in the proposed methodology.

6. Conclusions

The Montagna dei Fiori is an NNW-SSE trending overturned anticline within the Umbria-Marche succession. The SP52 road crosses the anticline in an East-West direction, encountering most of the geological formations of the Umbria Marche succession and often experiencing rockfall events.

The integration of field geomechanical and photogrammetric surveys has allowed the geomechanical characteristics of each geological formations outcropping in the back and upright for limbs of the Montagna dei Fiori anticline to be defined.

A new fast and low-cost method for creating photogrammetric models is presented based on the use of an object of known geometry and a geological compass. This can avoid the use of more expensive and often unavailable tools (i.e. total station) for scaling and georeferencing photogrammetric models. The data obtained using this simple methodology have been successfully validated against field measurements. This new approach is useful both for academic research and for engineering and geoscience practitioners when assessing the rockfall rock risk in vulnerable areas.

Two main joint sets, J1 (approx. ENE-WSW oriented) and J2 (approx. N-S oriented) characterize the anticline. The bedding planes are approximately N-S oriented and dip toward West in the backlimb of the anticline and to the West in the forelimb, with the dip varying from 20° to 80° in relation to the structural position on the anticline. Ji and Jv of the geological formation are strongly influenced by the lithology. In particular, geological formations characterized by limestone in thin beds or limestone alternating with marls present higher values of Jv and Ji. In more homogeneous formations of micrite limestone or calcarenites with thick beds (COI, MAI and MCERR Fms) lower Jv were measured.

Engineering rock mass classification has been carried out using the SMR classification system. Geomechanical and photogrammetric data were analyzed and improved through incorporation in GIS. Using this approach, it was possible to automatically calculate the SMR values for each section along the road in relation to the variation in rock slope attitude, geomechanical data and geology. Thematic GIS maps representing the most critical SMR values in the different sections of the SP52 road were developed. By reference to these GIS maps, calculated SMR values and Jv values, it was possible to define the most appropriate mitigation works according to Romana (1993).

A new method for defining the most appropriate mitigation work was proposed for geological formations characterized by the alternation of limestone and marls (i.e. RA and FUC). This new method is based on the kinematic relationships between marl layers and the rock slopes and the impact that such layers can have on the stability. The proposed method is intended as an extension to the existing SMR classification system for use in heterogeneous rock masses comprising alternating limestone and marls. The results of this research provide an additional tool for improving engineering decisions based on rock mass classification systems along highway and rail routes in folded terrain.

This paper presents a new method for engineering rock mass classification of natural slopes and road cuts. This multi-faceted method allows easy creation of 3D models of rock slopes and storage of all data in a GIS database. This approach optimizes data integration and analysis facilitating the definition of the most appropriate mitigation works. Such a fast and low-cost approach will provide increased benefits for engineers and geoscientists in improving the assessment of rockfall risk along major roads/railways.

References

- Abruzzi Regione open data 2018. http://opendata.regione.abruzzo.it/opendata/Modello_digitale_del_terreno_risoluzione_10x10_metri).
- Agisoft Photoscan (version 1.4). Agisoft (2018). http://www.agisoft.com/.
- Audisio C, Nigrelli G, Pasculli A, Sciarra N, Turconi L (2017) A GIS spatial analysis model for landslide hazard mapping application in Alpine Area. International Journal of Sustainable Development and Planning 12(5): 883-893.
- Badger TC (2002) Fracturing within anticlines and its kinematic control on slope stability. Environmental and Engineering Geoscience 8 (1): 19-33.
- Bar N, Barton N (2017) The Q-Slope method for rock slope engineering. Rock Mechanics and Rock Engineering 50 (12): 3307-3322.
- Barton NR, Lien R, Lunde J (1974) Engineering classification of rock masses for the design of tunnel support. Rock Mech 6(4): 189-239.
- Barton N, Grimstad E (2014) Tunnel and cavern support selection in Norway, based on rock mass classification with the Q-system. Norwegian Tunnelling Society 23: 45-77.
- Basahel H, Mitri H (2017) Application of rock mass classification systems to rock slope stability assessment: A case study. Journal of Rock Mechanics and Geotechnical Engineering 9: 993-1009.
- Bieniawski ZT (1973) Engineering classification of jointed rock masses. Trans. South Afr. Inst. of Civ. Eng 15 (12): 355-344.
- Bieniawski ZT (1989) Engineering Rock Mass Classifications. Wiley. New York.
- Bieniawski ZT (1993) Classification of rock masses for engineering: the RMR system and future trends. J.A. Hudson (Ed.), Comprehensive rock engineering: principles, practice and projects, Rock testing and site characterization, vol. 3, Pergamon, Oxford (1993), pp. 553-573.
- Budetta P, Nappi M (2011) Heterogeneous rock mass classification by means of the geological strength index: the San Mauro (Cilento, Italy). Bull. Eng Geol Environ 70: 585-593.
- Cai M, Kaiser PK, Uno H, Tasaka Y, Minami M (2004) Estimation of rock mass deformation modulus and strength of jointed hard rock masses using the GSI system. Int J Rock Mech Min Sci 41: 3-19.
- Calamita F, Pizzi A, Ridolfi M, Rusciadelli G, Scisciani V (1998) Il buttressing delle faglie sinsedimentarie pre-thrusting sulla strutturazione neogenica della catena appenninica: l'esempio della M.gna dei Fiori (Appennino Centrale esterno). Bollettino della Società Geologica Italiana 117: 725-745.
- Carminati E, Doglioni C (2012) Alps vs. Apennines: The paradigm of a tectonically asymmetric Earth. Earth-Science Reviews 112: 67-96.
- Cencetti C, Conversini P (2003) Slope instability in the Bastardo Basin (Umbria, Central Italy) – The landslide of Barattano. Natural Hazards and Earth System Sciences 3: 561-568.
- Chen Z (1995) Recent developments in slope stability analysis. In: Proceedings of the 8th international congress ISRM, Tokyo, 1995, p. 1041-8.
- CloudCompare (version 2.9), GPL software (2018). http://www.cloudcompare.org/.
- Day JJ, Diederichs MS, Hutchinson DJ (2014) Component and System Deformation Properties of Complex Rockmasses with Healed Structure. 48th U.S. Rock Mechanics/Geomechanics Symposium, 1-4 June, Minneapolis, Minnesota, 11 pp.
- Day JJ, Diederichs MS, Hutchinson DJ (2016) Validation of Composite Geological Strength Index for healed rockmass structure in deep mine access and production tunnels. Tunneling Association of Canada. 2016 annual conference, 16-14 October, Ottawa (CA).

- Di Francesco L, Fabbi S, Santantonio M, Bigi S, Poblet J (2010) Contribution of different kinematic models and a complex Jurassic stratigraphy in the construction of a forward model for the Montagna dei Fiori fault related fold (Central Apennines, Italy). Geological Journal 45: 489-505.
- Donati D, Stead D, Ghirotti M, Brideau MA (2017). A model-oriented, remote sensing approach for the derivation of numerical modelling input data: Insights from the Hope Slide, Canada. Proc. ISRM International Symposium 'Rock Mechanics for Africa' AfriRock Conference 2017, Cape Town, S., SAIMM, 15 pp.
- Francioni M, Salvini R, Stead D, Giovannini R, Riccucci S, Vanneschi C, Gullì D (2015) An integrated remote sensing-GIS approach for the analysis of an open pit in the Carrara marble district, Italy: Slope stability assessment through kinematic and numerical methods. Computers and Geotechnics 67: 46-63.
- Francioni M, Coggan J, Eyre M, Stead D (2018a) A combined field/remote sensing approach for characterizing landslide risk in coastal areas. International Journal of Applied Earth Observations and Geoinformation 67: 79-95.
- Francioni M, Stead D, Clague JJ, Westin A (2018b) Identification and analysis of large paleo-landslides at Mount Burnaby, British Columbia. Environ Eng Geosci 24 (2): 221-235.
- Francioni M, Salvini R, Stead D, Coggan JJ (2018c) Improvements in the integration of remote sensing and rock slope modelling. Natural Hazards 90: 975-1004.
- Hamidi JK, Shahriar K, Rezai B, Rostami J (2010) Performance prediction of hard rock TBM using Rock Mass Rating (RMR) system. Tunnelling and Underground Space Technology 25: 333-345.
- Hoek E (1994) Strength of rock and rock masses, ISRM News Journal 2 (2): 4-16.
- Hoek E, Kaiser PK, Bawden WF (1995) Support of underground excavations in hard rock. Rotterdam, Nether-lands: Balkema.
- Hoek E, Brown ET (1997) Practical estimates of rock mass strength. Int J Rock Mech Min Sci 34 (8): 1165-86.
- Hoek E, Marinos P (2000) Predicting Tunnel Squeezing. Tunnels and Tunnelling International 32(11): 45-51.
- Hoek E, Carter TG, Diederichs MS (2013) Quantification of the Geological Strength Index chart. 47th US Rock Mechanics/Geomechanics Symposium, AR-MA, San Francisco, 13-672.
- Jaques D, Rezende K, Marques E (2015) Rock mass classification applied to Volta Grande underground mine site in Brazil. Journal of Geological Resource and Engineering 4: 194-202.
- Marinos P, Hoek E (2000) GSI: a geologically friendly tool for rock mass strength estimation. In: Proceedings of the GeoEng2000, international conference on geotechnical and geological engineering, Melbourne, Technomic publishers, Lancaster, pp 1422-1446.
- Marinos P, Hoek E (2001). Estimating the geotechnical properties of heterogeneous rock masses such as flysch. Bull Eng Geol Env 60: 82-92
- Mattei M, (1987) Analisi geologico-strutturale della Montagna dei Fiori (Ascoli Piceno, Italia centrale). Geologica Romana 26: 327-347.
- McGinnis RN, Ferrill DA, Morris, A.P., Smart, K.J., Lehrmann, D. 2017. Mechanical stratigraphic controls on natural fracture spacing and penetration. Journal of Structural Geology, 95, 160-170.
- NGI - Norwegian Geotechnical Institute (2015) Using the Q system, handbook, 56pp. https://www.ngi.no/eng/Publications-and-library/Books/Q-system
- Pace P, Di Domenica A, Calamita F (2014) Summit low-angle faults in the Central Apennines of Italy: Younger-on-older thrusts or rotated normal faults? Constraints for defining the tectonic style of thrust belts. Tectonics 33: 756-785.

- Pantelidis L (2010) An alternative rock mass classification system for rock slopes. Bulletin of Engineering Geology and the Environment 69(1): 29-39.
- Price .J (1966) Fault and Joint Development in Brittle and Semi-brittle Rocks. Pergamon, Oxford.
- Regione Marche (2002) Piano regolatore portuale, Comune di Numana - relazione geologica, 27 pp. http://www.ambiente.marche.it/Portals/0/Territorio/Porti/numana/7_R_4_relazione_geologica.pdf
- Riquelme A, Tomás R, Abellán A (2014) SMRTool beta. A calculator for determining Slope Mass Rating (SMR). Universidad de Alicante. http://personal.ua.es/es/ariquelme/smrtool.html.
- Riquelme A, Tomás R, Abellán A (2016) Characterization of rock slopes through slope mass rating using 3D point clouds. International Journal of Rock Mechanics and Mining Sciences 84: 165-176.
- Romana MR (1985) New adjustment ratings for application of Bieniawski classification to slopes. In Proc. Int. Symp. On the Role of Rock Mech. pp 49-53. Zacatecas (1985).
- Romana MR (1993) A Geomechanical Classification for Slopes: Slope Mass Rating. Comprehensive Rock Engineering: Principles, Practice & Projects. Editor-in-Chief J. Hudson, Imperial College of Science, Technology & Medicine, London, UK, Volume 3: Rock Testing and Site Characterization.
- Romana MR, Serón JB, Montalar E (2003) SMR Geomechanics classification: Application, experience and validation. ISRM 2003–Technology roadmap for rock mechanics, South African Institute of Mining and Metallurgy.
- Romana MR, Tomas R, Seron JB (2015) Slope Mass Rating (SMR) geomechanics classification: thirty years review. 13th ISRM Congress Proceedings – International Symposium on Rock Mechanics, Quebec, Canada, May 10 to 13, 2015, 10 pp.
- Salvini R, Francioni M, Fantozzi PL, Riccucci S, Bonciani F, Mancini S (2011) Stability analysis of “Grotta delle Felci” Cliff (Capri Island, Italy): structural, engineering–geological, photogrammetric surveys and laser scanning. Bull. Eng Geol Environ 70: 549-557.
- Salvini R, Francioni M, Riccucci S, Bonciani F, Callegari I (2013) Photogrammetry and laser scanning for analyzing slope stability and rock fall runout along the Domodossola–Iselle railway, the Italian Alps. Geomorphology 185: 110-122.
- Sciarra N, Marchetti D, D'Amato Avanzi G, Calista M (2015) Rock slope analysis on the complex livorno coastal cliff (Tuscany, Italy). Geografia Fisica e Dinamica Quaternaria 37 (2): 113-130.
- Scisciani V, Tavarnelli E, Calamita F, (2002) The interaction of extensional and contractional deformations in the outer zones of the Central Apennines, Italy. Journal of Structural Geology 24: 1647-1658.
- Scisciani V, Montefalcone R (2006) Coexistence of thin- and thick-skinned tectonics: An example from the Central Apennines, Italy. In Mazzoli S, and Butler RWH, eds., Styles of Continental Contraction: Geological Society of America Special Paper 414: 33-54.
- Scisciani V, Agostini S, Calamita F, Pace P, Cilli A, Giori I, Paltrinieri W (2014) Positive inversion tectonics in foreland fold-and thrust belts: A reappraisal of the Umbria–Marche Northern Apennines (Central Italy) by integrating geological and geophysical data.Tectonophysics 637: 218-237.
- Stead D, Wolter A (2015) A critical review of rock slope failure mechanisms: The importance of structural geology. Journal of Structural Geology 74: 1-23.
- Storti F, Balsamo F, Koopman A (2016) Geological map of the partially dolomitized Jurassic succession exposed in the central sector of the Montagna dei Fiori Anticline, Central Apennines, Italy. Italian Journal of Geoscience 136: 1-35.

- Sturzenegger M, Stead D (2009) Close-range terrestrial digital photogrammetry and terrestrial laser scanning for discontinuity characterization on rock cuts. Engineering Geology 106: 163-182.
- Tavarnelli E (1996a) Ancient synsedimentary structural control on thrust ramp development: An example from the Northern Apennines, Italy. Terra Nova 8: 65-74.
- Tavarnelli E (1996b) The effects of pre-existing normal faults on thrust ramp development: An example from the northern Apennines, Italy. Geology of Earth Science Research 85: 363-371.
- Tavarnelli E, Peacock DCP (1999) From extension to contraction in syn-orogenic foredeep basins: The Contessa section, Umbria-Marche Apennines, Italy. Terra Nova 11: 55-60.
- Tomás R, Delgado J, Serón JB (2007) Modification of slope mass rating (SMR) by continuous functions. International Journal of Rock Mechanics and Mining Sciences 44: 1062-1069.
- Tomás R, Cuenca A, Cano M, Garcßa-Barbra J (2012) A graphical approach for slope mass rating (SMR). Engineering Geology 124 (4): 67-76.
- Van Westen CJ (1998) GIS in landslide hazard zonation: A view, with cases from the Andes of Colombia. In: Mountain Environment and Geographic Information Systems, F.P. Martin, D.I. Heywood (eds.). Taylor & Francis, London, pp. 35-165.
- Watkins H, Butler RWH (2017) Implications of heterogeneous fracture distribution on reservoir quality: an analogue from the Torridon Group sandstone, Moine Thrust Belt, NW Scotland. Journal of Structural Geology 108: 180-197.
- Westoby MJ, Brasington J, Glasser NF, Hambrey MJ, Reynolds JM (2012) 'Structure-from-Motion' photogrammetry: a low-cost, effective tool for geoscience. Geomorphology 179: 300-314.
- Wu C (2011) VisualSFM: A Visual Structure from Motion System, http://www.cs.washington.edu/homes/ccwu/vsfm/
- Wolter A, Stead D, Ward BC, Clague JJ, Ghirotti M (2016) Engineering geomorphological characterisation of the Vajont Slide, Italy, and a new interpretation of the chronology and evolution of the landslide. Landslides 5: 1067-1081.
- Xie M, Esaki T, Qiu C, Wang CX (2006) Geographical information system-based computational implementation and application of spatial three-dimensional slope stability analysis. Computers and Geotechnics 33: 260-274.
- Yilmaz I, Marschalko M, Yildirim M, Dereli E, Bednarik M (2012) GIS-based kinematic slope instability and slope mass rating (SMR) maps: application to a railway route in Sivas (Turkey). Bulletin of Engineering Geology and the Environment 71 (2): 351-357.